THE EUROPEAN
PHYSICAL JOURNAL C

CrossMark

Regular Article - Experimental Physics

Measurement of the top quark mass with lepton+jets final states using pp collisions at $\sqrt{s} = 13$ TeV

CMS Collaboration[*]

CERN, 1211 Geneva 23, Switzerland

Abstract The mass of the top quark is measured using a sample of $t\bar{t}$ events collected by the CMS detector using proton-proton collisions at $\sqrt{s} = 13$ TeV at the CERN LHC. Events are selected with one isolated muon or electron and at least four jets from data corresponding to an integrated luminosity of $35.9\,\text{fb}^{-1}$. For each event the mass is reconstructed from a kinematic fit of the decay products to a $t\bar{t}$ hypothesis. Using the ideogram method, the top quark mass is determined simultaneously with an overall jet energy scale factor (JSF), constrained by the mass of the W boson in $q\bar{q}'$ decays. The measurement is calibrated on samples simulated at next-to-leading order matched to a leading-order parton shower. The top quark mass is found to be $172.25 \pm 0.08\,\text{(stat+JSF)} \pm 0.62\,\text{(syst)}$ GeV. The dependence of this result on the kinematic properties of the event is studied and compared to predictions of different models of $t\bar{t}$ production, and no indications of a bias in the measurements are observed.

1 Introduction

The top quark plays a key role in precision measurements of the standard model (SM) because of its large Yukawa coupling to the Higgs boson. Top quark loops provide the dominant contribution to radiative corrections to the Higgs boson mass, and accurate measurements of both the top quark mass (m_t) and the Higgs boson mass allow consistency tests of the SM [1]. In addition, the decision whether the SM vacuum is stable or meta-stable needs a precise measurement of m_t as the Higgs boson quartic coupling at the Planck scale depends heavily on m_t [2].

The mass of the top quark has been measured with increasing precision using the invariant mass of different combinations of its decay products [3]. The measurements by the Tevatron collaborations lead to a combined value of $m_t = 174.30 \pm 0.65$ GeV [4], while the ATLAS and CMS Collaborations measured $m_t = 172.84 \pm 0.70$ GeV [5] and $m_t = 172.44 \pm 0.49$ GeV [6], respectively, from the combination of their most precise results. In parallel, the theoretical interpretation of the measurements and the uncertainties in the measured top quark mass derived from the modeling of the selected variables has significantly improved [7–13].

Since the publication of the CMS measurements [6] for proton-proton (pp) collisions at center-of-mass energies of 7 and 8 TeV (Run 1), new theoretical models have become available and a data set has been collected at $\sqrt{s} = 13$ TeV that is larger than the Run 1 data set. At this higher center-of-mass energy, new data and simulated samples are available for this analysis. The method closely follows the strategy of the most precise CMS Run 1 measurement [6]. While the selected final state, the kinematic reconstruction, and mass extraction technique have not changed, the new simulations describe the data better and allow a more refined estimation of the modeling uncertainties. In contrast to the Run 1 analysis, the renormalization and factorization scales in the matrix-element (ME) calculation and the scales in the initial- and final-state parton showers (PS) are now varied separately for the evaluation of systematic effects. In addition, we evaluate the impact of different models of color reconnection that were not available for the Run 1 measurements.

The pair-produced top quarks ($t\bar{t}$) are assumed to decay weakly into W bosons and bottom (b) quarks via $t \rightarrow bW$, with one W boson decaying into a muon or electron and its neutrino, and the other into a quark–antiquark ($q\bar{q}'$) pair. Hence, the minimal final state consists of a muon or electron, at least four jets, and one undetected neutrino. This includes events where a muon or electron from a τ lepton decay passes the selection criteria. The analysis employs a kinematic fit of the decay products to a $t\bar{t}$ hypothesis and two-dimensional likelihood functions for each event to estimate simultaneously the top quark mass and a scale factor (JSF) to be applied to the momenta of all jets. The invariant mass of the two jets associated with the $W \rightarrow q\bar{q}'$ decay serves as

an observable in the likelihood functions to estimate the JSF directly, exploiting the precise knowledge of the W boson mass from previous measurements [3]. The analysis is performed on the data sample collected in 2016 and includes studies of the dependence of the measured mass value on the kinematic properties of the events.

2 The CMS detector and event reconstruction

The central feature of the CMS apparatus is a superconducting solenoid of 6 m internal diameter, providing a magnetic field of 3.8 T. Within the solenoid volume are a silicon pixel and strip tracker, a lead tungstate crystal electromagnetic calorimeter (ECAL), and a brass and scintillator hadron calorimeter (HCAL), each composed of a barrel and two endcap sections. Forward calorimeters extend the pseudorapidity (η) coverage provided by the barrel and endcap detectors. Muons are detected in gas-ionization chambers embedded in the steel flux-return yoke outside the solenoid. A more detailed description of the CMS detector, together with a definition of the coordinate system used and the relevant kinematic variables, can be found in Ref. [14].

The particle-flow event algorithm [15] reconstructs and identifies each individual particle with an optimized combination of information from the various elements of the CMS detector. The energy of photons is directly obtained from the ECAL measurement, corrected for zero-suppression effects. The energy of electrons is determined from a combination of the electron momentum at the primary interaction vertex as determined by the tracker, the energy of the corresponding ECAL cluster, and the energy sum of all bremsstrahlung photons spatially compatible with originating from the electron track. The energy of muons is obtained from the curvature of the corresponding track. The energy of charged hadrons is determined from a combination of their momentum measured in the tracker and the matching ECAL and HCAL energy deposits, corrected for zero-suppression effects and for the response function of the calorimeters to hadronic showers. Finally, the energy of neutral hadrons is obtained from the corresponding corrected ECAL and HCAL energy.

The missing transverse momentum $\vec{p}_{\mathrm{T}}^{\mathrm{miss}}$ is calculated as the negative of the vectorial sum of transverse momenta (p_{T}) of all particle-flow objects in the event. Jets are clustered from particle-flow objects using the anti-k_{T} algorithm with a distance parameter of 0.4 [16–18]. The jet momentum is determined as the vectorial sum of all particle momenta in the jet, and is found from simulation to be within 5 to 10% of the true momentum over the whole p_{T} spectrum and detector acceptance. An offset correction is applied to jet energies to take into account the contribution from additional pp interactions within the same or nearby bunch crossings (pileup) [19]. All jets are corrected by jet energy correc-

tions (JECs) based on simulations. Residual JECs which are derived from the energy balance in γ/Z boson + jet, dijet, and multijet events [20] are applied to the jets in data. The JECs are also propagated to improve the measurement of $\vec{p}_{\mathrm{T}}^{\mathrm{miss}}$. The reconstructed vertex with the largest value of summed physics-object p_{T}^2 is taken to be the primary pp interaction vertex. The physics objects chosen are those that have been defined using information from the tracking detector, including jets, $\vec{p}_{\mathrm{T}}^{\mathrm{miss}}$, and charged leptons. Additional selection criteria are applied to each event to remove spurious jet-like features originating from isolated noise patterns in certain HCAL regions [21].

3 Data samples, event generation, and selection

The data sample collected with the CMS detector during 2016 at a center-of-mass energy $\sqrt{s} = 13$ TeV has been analyzed. This corresponds to an integrated luminosity of $35.9 \pm 0.9\,\mathrm{fb}^{-1}$ [22]. Events are required to pass a single-muon trigger with a minimum threshold on the p_{T} of an isolated muon of 24 GeV or a single-electron trigger with a p_{T} threshold for isolated electrons of 32 GeV.

Simulated $t\bar{t}$ signal events are generated at next-to-leading order (NLO) with POWHEG v2 [23–26] and the PYTHIA 8.219 PS generator [27] using the CUETP8M2T4 tune [28,29] for seven different top quark mass values of 166.5, 169.5, 171.5, 172.5, 173.5, 175.5, and 178.5 GeV. The single top quark background is also simulated using POWHEG v2 [30,31] interfaced with PYTHIA 8. The background stemming from single vector boson production is generated at leading order (LO) or NLO with MADGRAPH5_aMC@NLO v2.2.2 [32] matched to the PYTHIA 8 PS using the MLM prescription [33] for W+jets and the FxFx prescription [34] for Z+jets, respectively. Finally, diboson (WW, WZ, and ZZ) and multijet events from quantum chromodynamics (QCD) processes are generated with PYTHIA 8 for ME generation, PS simulation, and hadronization. These background samples use the PYTHIA 8 tune CUETP8M1. The parton distribution function (PDF) set NNPDF3.0 NLO derived with the strong coupling strength $\alpha_S = 0.118$ [35] and its corresponding LO version are used as the default parametrization of the PDFs in all simulations, respectively. The samples are normalized to the theoretical predictions described in Refs. [27,36–39]. All events are further processed by a full simulation of the CMS detector based on GEANT4 [40]. The simulation includes effects of pileup with the same multiplicity distribution as in data. The response and the resolution of simulated jets is corrected to match the data [20].

We select events that have exactly one isolated muon with $p_{\mathrm{T}} > 26$ GeV and $|\eta| < 2.4$ or exactly one isolated electron with $p_{\mathrm{T}} > 34$ GeV and $|\eta| < 2.1$ [41,42]. The isolation of a lepton candidate from nearby jet activity is evaluated
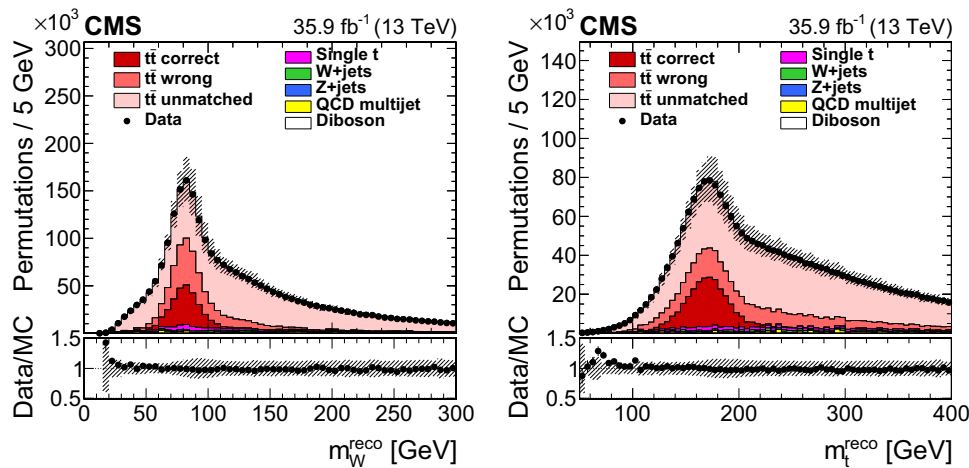
Fig. 1 Invariant mass m_W^{reco} of the two untagged jets (left) and invariant mass m_t^{reco} of the two untagged jets and one of the b-tagged jets (right) after the b tagging requirement. For the simulated $t\bar{t}$ events, the jet-parton assignments are classified as correct, wrong, and unmatched permutations as described in the text. The vertical bars show the statistical uncertainty on the data and the hatched bands show the systematic uncertainties considered in Sect. 5. The lower portion of each panel shows the ratio of the yields between data and the simulation. The simulations are normalized to the integrated luminosity

from the sum of the pileup-corrected p_T of neutral hadrons, charged hadrons, and photon PF candidates within a cone of $\Delta R = \sqrt{(\Delta\eta)^2 + (\Delta\phi)^2} = 0.4$ for muons and $\Delta R = 0.3$ for electrons. Here $\Delta\eta$ and $\Delta\phi$ are the differences in the pseudorapidity and azimuthal angles (in radians) between the particles and the lepton candidate. The sum of the p_T of the particles is required to be less than 15% of the muon p_T and 10% of the electron p_T, respectively.

In addition, at least four jets with $p_T > 30$ GeV and $|\eta| < 2.4$ are required. Only the four leading among the jets passing these p_T- and η-criteria are used in the reconstruction of the $t\bar{t}$ system. Jets originating from b quarks are identified (tagged) using an algorithm that combines reconstructed secondary vertices and track-based lifetime information. This has an efficiency of approximately 70% and a mistagging probability for light-quark and gluon jets of 1% [43]. We require exactly two b-tagged jets among the four leading ones and select 669,109 $t\bar{t}$ candidate events in data. Figure 1 shows the distributions of the reconstructed mass m_W^{reco} of the W boson decaying to a $q\bar{q}'$ pair and the masses m_t^{reco} computed from the two untagged jets and each of the two b-tagged jets at this selection step. For simulated $t\bar{t}$ events, the parton-jet assignments can be classified as correct permutations (*cp*), wrong permutations (*wp*), and unmatched permutations (*un*), where, in the latter, at least one quark from the $t\bar{t}$ decay is not unambiguously matched within a distance of $\Delta R < 0.4$ to any of the four selected jets.

To check the compatibility of an event with the $t\bar{t}$ hypothesis, and to improve the resolution of the reconstructed quantities, a kinematic fit [44] is performed. For each event, the inputs to the algorithm are the four-momenta of the lepton and of the four leading jets, $\vec{p}_T^{miss}$, and the resolutions of these

variables. The fit constrains these quantities to the hypothesis that two heavy particles of equal mass are produced, each one decaying to a bottom quark and a W boson, with the invariant mass of the latter constrained to 80.4 GeV. The kinematic fit then minimizes $\chi^2 \equiv (\mathbf{x} - \mathbf{x}^m)^T G (\mathbf{x} - \mathbf{x}^m)$ where $\mathbf{x}^m$ and $\mathbf{x}$ are the vectors of the measured and fitted momenta, respectively, and G is the inverse covariance matrix which is constructed from the uncertainties in the measured momenta. The two b-tagged jets are candidates for the b quarks in the $t\bar{t}$ hypothesis, while the two untagged jets serve as candidates for the light quarks from the hadronically decaying W boson. This leads to two possible parton-jet assignments with two solutions for the longitudinal component of the neutrino momentum each, resulting in four different permutations per event.

To increase the fraction of correct permutations, we require the goodness-of-fit (gof) probability for the kinematic fit with two degrees of freedom $P_{gof} = \exp(-\chi^2/2)$ to be at least 0.2. This requirement selects 161 496 events in data, while the non-$t\bar{t}$ background in the simulated data is reduced from 7.6 to 4.3%. The remaining background consists mostly of single top quark events (2.5%). Any of the four permutations in an event that passes the selection criteria is weighted by its P_{gof} value and is used in the measurement. These steps improve the fraction of correct permutations from 14.9 to 48.0%. Figure 2 shows the final distributions after the P_{gof} selection of the reconstructed mass m_W^{reco} of the W boson decaying to a $q\bar{q}'$ pair and the invariant mass of the top quark candidates from the kinematic fit m_t^{fit} for all selected permutations. These two observables are used in the mass extraction.

Fig. 2 Reconstructed W boson masses m_W^{reco} (left) and fitted top quark masses m_t^{fit} (right) after the goodness-of-fit selection and the weighting by P_{gof}. Symbols and patterns are the same as in Fig. 1. The simulations are normalized to the integrated luminosity
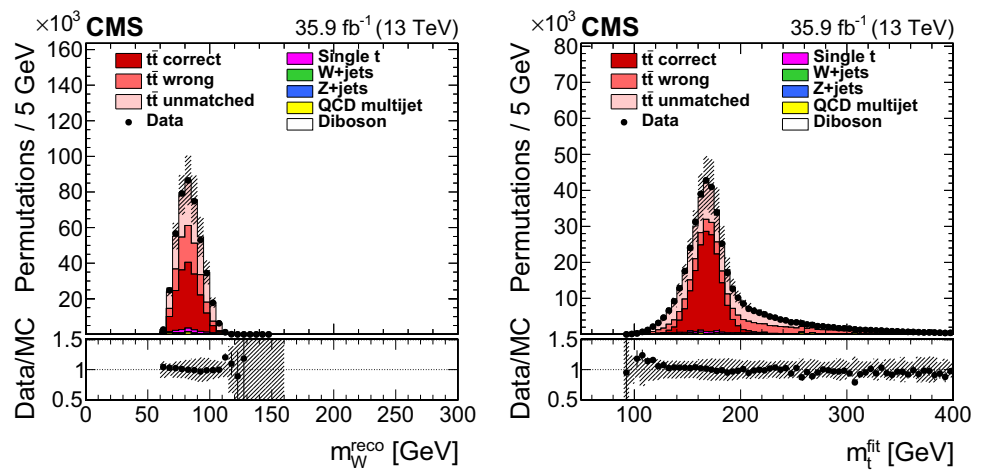
4 Ideogram method

An ideogram method [45] is employed as described in Ref. [46]. The details of the procedure outlined below are identical with the approach taken in the Run 1 CMS measurement [6]. The observable used to measure m_t is the mass m_t^{fit} evaluated after applying the kinematic fit. We take the reconstructed W boson mass m_W^{reco}, before it is constrained by the kinematic fit, as an estimator for measuring the JSF to be applied in addition to the standard CMS JECs. The top quark mass and the JSF are determined simultaneously in a likelihood fit to the selected permutations, in order to reduce the uncertainty from the JECs.

The distributions of m_t^{fit} and m_W^{reco} are obtained from simulation for seven different m_t and five different JSF values. From these distributions, probability density functions P_j are derived separately for the different permutation cases j: cp, wp, or un. These functions depend on m_t and the JSF and are labeled $P_j(m_{t,i}^{fit}|m_t, \mathrm{JSF})$ and $P_j(m_{W,i}^{reco}|m_t, \mathrm{JSF})$, respectively, for the ith permutation of an event in the final likelihood. The observables m_t^{fit} and m_W^{reco} have a correlation coefficient with a size below 5% for each permutation case and are treated as uncorrelated. The most likely m_t and JSF values are obtained by minimizing $-2 \ln\left[\mathcal{L}\left(\text{sample}|m_t, \mathrm{JSF}\right)\right]$. With an additional prior $P(\mathrm{JSF})$, the likelihood $\mathcal{L}\left(\text{sample}|m_t, \mathrm{JSF}\right)$ is defined as:

$$
\begin{aligned}
\mathcal{L}\left(\text{sample}|m_t, \mathrm{JSF}\right) = {} & P(\mathrm{JSF}) \prod_{\text{events}} \left(\sum_{i=1}^{n} P_{gof}(i) \right. \\
& \times \left. \left[\sum_j f_j\, P_j(m_{t,i}^{fit}|m_t, \mathrm{JSF})\, P_j(m_{W,i}^{reco}|m_t, \mathrm{JSF}) \right] \right)^{w_{evt}},
\end{aligned}
$$

where n denotes the number of the at-most four permutations in each event, j labels the permutation cases, and f_j represents their relative fractions. The event weight $w_{evt} = c \sum_{i=1}^{n} P_{gof}(i)$ is introduced to reduce the impact of events

without correct permutations, where c normalizes the average w_{evt} to 1.

Different choices are made for the prior $P(\mathrm{JSF})$ in the likelihood fit. When the JSF is fixed to unity, the $P_j(m_{W,i}^{reco}|m_t, \mathrm{JSF})$ can be approximated by a constant as they hardly depend on m_t. Hence, only the m_t^{fit} observable is fit, and this approach is called the 1D analysis. The approach with an unconstrained JSF is called the 2D analysis. Finally, in the hybrid analysis, the prior $P(\mathrm{JSF})$ is a Gaussian centered at 1.0. Its width depends on the relative weight w_{hyb} that is assigned to the prior knowledge on the JSF, $\sigma_{prior} = \delta \mathrm{JSF}_{stat}^{2D}\sqrt{1/w_{hyb} - 1}$, where $\delta \mathrm{JSF}_{stat}^{2D}$ is the statistical uncertainty in the 2D result of the JSF. The optimal value of w_{hyb} is determined from the uncertainties in the 2D analysis and discussed in Sect. 5.

The 2D method is separately calibrated for the muon and electron channel by conducting 10,000 pseudo-experiments for each combination of the seven top quark masses and the five JSF values, using simulated $t\bar{t}$ and background events. We correct for deviations between the extracted mass and JSF and their input values. This bias correction amounts for the mass to an offset of 0.5 GeV for an expected value of 172.5 GeV, with a slope of 3%. Corrections for the statistical uncertainty of the method are derived from the widths of the corresponding pull distributions and have a size of 5% for both the mass and the JSF.

5 Systematic uncertainties

The systematic uncertainties in the final measurement are determined from pseudo-experiments. Taking into account new simulations, more variations of the modeling of the $t\bar{t}$ events are investigated than in the Run 1 analysis [6]. The scales used for the simulation of initial-state radiation (ISR) and final-state radiation (FSR) are varied independently from the renormalization and factorization scales. Furthermore, the effects of early resonance decays and alternative color-

reconnection models [47,48] are evaluated, while in Run 1 only the effect of an underlying event tune without color reconnection was studied. The relevant systematic uncertainties and the methods used to evaluate them are described below.

Method calibration: We consider the quadratic sum of statistical uncertainty and residual biases after the calibration of the ideogram method as a systematic uncertainty.

JECs: As we measure a global JSF, we have to take into account the influence of the p_T- and η-dependent JEC uncertainties. This is done by scaling the energies of all jets up and down according to their individual uncertainties [20], split into correlation groups (called InterCalibration, MPFInSitu and Uncorrelated) similarly to the procedure adopted at 8 TeV [49].

Jet energy resolution: The jet energy resolution (JER) in simulation is slightly degraded to match the resolutions measured in data [20]. To account for the resolution uncertainty, the JER in the simulation is modified by ± 1 standard deviation with respect to the degraded resolution.

b *tagging*: The events are weighted to account for the p_T-dependent uncertainty of the b tagging efficiencies and misidentification rates of the b tagging algorithm [43].

Pileup: To estimate the uncertainties associated with the determination of the number of pileup events and with the weighting procedure, the inelastic pp cross section is varied by $\pm 4.6\%$ for all simulations.

Non-t$\bar{\text{t}}$ background: The main uncertainty in the non-t$\bar{\text{t}}$ background stems from the uncertainty in the measurements of the cross sections used in the normalization. The normalization of the background samples is varied by $\pm 10\%$ for the single top quark samples [50,51], $\pm 30\%$ for the W+jets samples [52], $\pm 10\%$ for the Z+jets [53] and for the diboson samples [54,55], and $\pm 100\%$ for the QCD multijet samples. The uncertainty in the luminosity of 2.5% [22] is negligible compared to these variations.

JEC Flavor: The Lund string fragmentation implemented in PYTHIA 6.422 [56] is compared to the cluster fragmentation of HERWIG++ 2.4 [57]. Each model relies on a large set of tuning parameters that allow to modify the individual fragmentation of jets initiated from gluons, light quarks, and b quarks. Therefore, the difference in jet energy response between PYTHIA 6 and HERWIG++ is determined for each jet flavor [20]. In order to evaluate possible differences between the measured JSF (from light quarks with gluon contamination) and the b jet energy scale, the flavor uncertainties for jets from light quarks, gluons, and bottom quarks are evaluated separately and added linearly.

b *jet modeling*: This term has three components: The fragmentation into b hadrons is varied in simulation within the uncertainties of the Bowler–Lund fragmentation function tuned to ALEPH [58] and DELPHI [59] data. In addition, the difference between the Bowler–Lund [60] and the Peter-

son [61] fragmentation functions is included in the uncertainty. Lastly, the uncertainty from the semileptonic b hadron branching fraction is obtained by varying it by -0.45% and $+0.77\%$, which is the range of the measurements from B^0/B^+ decays and their uncertainties [3].

PDFs: The NNPDF3.0 NLO ($\alpha_S = 0.118$) PDF is used in the generation of simulated events. We calculate the results with the different PDF replicas and use the variance of these predictions for the PDF uncertainty [35]. In addition, NNPDF3.0 sets with $\alpha_S = 0.117$ and 0.119 are evaluated and the observed difference is added in quadrature [62–64].

Renormalization and factorization scales: The simulated events are weighted to match the event shape distributions generated with different renormalization and factorization scales. These scales are varied independently from each other by a factor of 0.5 and 2.

ME/PS matching: The model parameter $h_{\text{damp}} = 1.58^{+0.66}_{-0.59}$ [29] used in POWHEG to control the matching of the MEs to the PYTHIA 8 PS is varied within its uncertainties.

ME generator: The influence of the NLO ME generator and its matching to the PS generator is estimated by using a sample from the NLO generator MADGRAPH5_aMC@NLO with FxFx matching [34], instead of the POWHEG v2 generator used as default.

ISR PS scale: The PS scale value used for the simulation of ISR in PYTHIA 8 is scaled up by 2 and down by 0.5 in dedicated samples.

FSR PS scale: The PS scale value used for the simulation of FSR in PYTHIA 8 is scaled up by $\sqrt{2}$ and down by $1/\sqrt{2}$ [28] in dedicated samples. This affects the fragmentation and hadronization of the jets initiated by the ME calculation, as well as the emission of extra jets. In the FSR samples, the jet energy response of the light quarks is observed to differ by $\pm 1.2\%$ compared to the response of the default sample. This response difference would be absorbed in the residual JECs if the corrections were derived based on γ/Z+jet simulations with the same PS scale. Hence, the momenta of all jets in the varied samples are scaled so that the energy response for jets induced by light quarks agrees with the default sample.

Top quark p_T: Recent calculations [65] suggest that next-to-next-to-leading-order effects have an important impact on the top quark p_T spectrum, that NLO ME generators are unable to reproduce. Therefore, the top quark p_T in simulation is varied to match the distribution measured by CMS [66,67]. The observed difference with respect to the default sample is quoted as a systematic uncertainty.

Underlying event: The modeling of multiple-parton interactions in PYTHIA 8 is tuned to measurements of the underlying event [28,29]. The parameters of the tune are varied within their uncertainties in the simulation of the t$\bar{\text{t}}$ signal.

Early resonance decays: By enabling early resonance decays (ERDs) in PYTHIA 8, color reconnections can hap-

Table 1 Observed shifts with respect to the default simulation for different models of color reconnection. The "QCD inspired" and "gluon move" models are compared to the default model with ERDs. The statistical uncertainty in the JSF shifts is 0.1%

	2D approach		1D approach	Hybrid	
	$\delta m_{\mathrm{t}}^{\mathrm{2D}}$ [GeV]	δJSF$^{\mathrm{2D}}$ [%]	$\delta m_{\mathrm{t}}^{\mathrm{1D}}$ [GeV]	$\delta m_{\mathrm{t}}^{\mathrm{hyb}}$ [GeV]	δJSF$^{\mathrm{hyb}}$ [%]
POWHEG P8 ERD on	-0.22 ± 0.09	$+0.8$	$+0.42 \pm 0.05$	-0.03 ± 0.07	$+0.5$
POWHEG P8 QCD inspired	-0.11 ± 0.09	-0.1	-0.19 ± 0.06	-0.13 ± 0.08	-0.1
POWHEG P8 gluon move	$+0.34 \pm 0.09$	-0.1	$+0.23 \pm 0.06$	$+0.31 \pm 0.08$	-0.1

Table 2 Observed shifts with respect to the default simulation for different generator setups. The statistical uncertainty in the JSF shifts is 0.1%

	2D approach		1D approach	Hybrid	
	δm_t^{2D} [GeV]	δJSF$^{\mathrm{2D}}$ [%]	δm_t^{1D} [GeV]	$\delta m_t^{\mathrm{hyb}}$ [GeV]	δJSF$^{\mathrm{hyb}}$ [%]
MG5 P8 [FxFx] M2T4	$+0.15 \pm 0.23$	$+0.2$	$+0.32 \pm 0.14$	$+0.20 \pm 0.19$	$+0.1$
MG5 P8 [MLM] M1	$+0.82 \pm 0.16$	< 0.1	$+0.80 \pm 0.10$	$+0.82 \pm 0.14$	< 0.1
POWHEG H++ EE5C	-4.39 ± 0.09	$+1.4$	-3.26 ± 0.06	-4.06 ± 0.08	$+1.0$

pen between particles from the top quark decay and particles from the underlying event. In the default sample the ERDs are turned off and the top quark decay products do not interact with the underlying event. The influence of the ERD setting is estimated from a sample with ERDs enabled in PYTHIA 8.

Color reconnection: The uncertainties that arise from ambiguities in modeling color-reconnection effects are estimated by comparing the default model in PYTHIA 8 with ERDs to two alternative models of color reconnection, a model with string formation beyond leading color ("QCD inspired") [48] and a model that allows gluons to be moved to another string ("gluon move") [47]. All models are tuned to measurements of the underlying event [28,68]. The observed shifts are listed in Table 1. Among the two approaches, the "gluon move" model leads to larger shifts and these are quoted as the systematic uncertainty.

The modeling uncertainties are mainly evaluated by varying the parameters within one model: POWHEG v2 + PYTHIA 8 with the CUETP8M2T4 tune (labeled as POWHEG P8 M2T4). This approach benefits from the calibration of the reconstructed physics objects which is derived from data with PYTHIA 8 as a reference. Three alternative models of the $t\bar{t}$ signal are studied. The NLO MADGRAPH5_aMC@NLO generator with the FxFx matching [34] (labeled as MG5 P8 [FxFx] M2T4) and the LO MADGRAPH5_aMC@NLO with the MLM matching [33] (labeled as MG5 P8 [MLM] M1) are both interfaced with PYTHIA 8 with the CUETP8M2T4 and the CUETP8M1 tune, respectively. In addition, POWHEG v2 interfaced with HERWIG++ [57] (v2.7.1) with the tune EE5C [69] (labeled as POWHEG H++ EE5C) is evaluated. ME corrections to the top quark decay are not applied in the HERWIG++ sample. A dedicated analysis has found that MG5 P8 [MLM] M1 and POWHEG H++ EE5C do not describe the data

well [29,70] and only the NLO MG5 P8 [FxFx] M2T4 model is used in the evaluation of the systematic uncertainties.

Nevertheless, the analysis is also performed on pseudo-experiments where the $t\bar{t}$ signal stems from these different generator setups. This yields rather large shifts for the two discarded models. The results are summarized in Table 2. The shift for POWHEG H++ EE5C would translate into a 4 GeV higher measurement of m_{t} if this setup were used as the default $t\bar{t}$ simulation and not as signal in the pseudo-data. The agreement of these generator setups and the color-reconnection models with data are studied in Sect. 7 for this top quark mass measurement.

The contributions from the different sources of systematic uncertainties are shown in Table 3. In general, the absolute value of the largest observed shifts in m_{t} and JSF, determined by changing the parameters by ± 1 standard deviation (σ), are assigned as systematic uncertainties. The only exception to this is if the statistical uncertainty in the observed shift is larger than the value of the calculated shift. In this case the statistical uncertainty is taken as the best estimate of the uncertainty in the parameter. The signs in the table are taken from the $+1\sigma$ shift in the value of the uncertainty source where applicable.

The details of the fitting procedure have several consequences on the uncertainties. The inclusion of the JSF as a nuisance parameter in the fit and its constraint by the $m_{\mathrm{W}}^{\mathrm{reco}}$ observable reduces not only the uncertainties stemming from the JECs, but also the modeling uncertainties. As the JSF is an overall energy scale factor derived mainly on light-quark jets and applied to all jets, this approach cannot reduce the uncertainties on the flavor-dependent JECs. The other remaining systematic uncertainties are also dominated by effects that cannot be fully compensated through the simultaneous deter-

Table 3 List of systematic uncertainties for the fits to the combined data set using the procedures described in Sect. 5. With the exception of the flavor-dependent JEC terms, the total systematic uncertainty is obtained from the sum in quadrature of the individual systematic uncertainties. The values in parentheses with indented labels are already included in the preceding uncertainty source. A positive sign indicates an increase in the value of m_t or the JSF in response to a $+1\sigma$ shift and a negative sign indicates a decrease. The statistical uncertainty in the shift in m_t is given when different samples are compared. The statistical uncertainty in the JSF shifts is 0.1% for these sources

	2D approach		1D approach	Hybrid	
	δm_t^{2D} [GeV]	δJSF^{2D} [%]	δm_t^{1D} [GeV]	δm_t^{hyb} [GeV]	δJSF^{hyb} [%]
Experimental uncertainties					
Method calibration	0.05	< 0.1	0.05	0.05	< 0.1
JEC (quad. sum)	0.13	0.2	0.83	0.18	0.3
– InterCalibration	(− 0.02)	(< 0.1)	(+ 0.16)	(+ 0.04)	(< 0.1)
– MPFInSitu	(− 0.01)	(< 0.1)	(+ 0.23)	(+ 0.07)	(< 0.1)
– Uncorrelated	(− 0.13)	(+ 0.2)	(+ 0.78)	(+ 0.16)	(+ 0.3)
Jet energy resolution	− 0.20	+ 0.3	+ 0.09	− 0.12	+ 0.2
b tagging	+ 0.03	< 0.1	+ 0.01	+ 0.03	< 0.1
Pileup	− 0.08	+ 0.1	+ 0.02	− 0.05	+ 0.1
Non-$t\bar{t}$ background	+ 0.04	− 0.1	− 0.02	+ 0.02	− 0.1
Modeling uncertainties					
JEC Flavor (linear sum)	− 0.42	+ 0.1	− 0.31	− 0.39	< 0.1
– light quarks (uds)	(+ 0.10)	(− 0.1)	(− 0.01)	(+ 0.06)	(− 0.1)
– charm	(+ 0.02)	(< 0.1)	(− 0.01)	(+ 0.01)	(< 0.1)
– bottom	(− 0.32)	(< 0.1)	(− 0.31)	(− 0.32)	(< 0.1)
– gluon	(− 0.22)	(+ 0.3)	(+ 0.02)	(− 0.15)	(+ 0.2)
b jet modeling (quad. sum)	0.13	0.1	0.09	0.12	< 0.1
– b frag. Bowler–Lund	(− 0.07)	(+ 0.1)	(− 0.01)	(− 0.05)	(< 0.1)
– b frag. Peterson	(+ 0.04)	(< 0.1)	(+ 0.05)	(+ 0.04)	(< 0.1)
– semileptonic B decays	(+ 0.11)	(< 0.1)	(+ 0.08)	(+ 0.10)	(< 0.1)
PDF	0.02	< 0.1	0.02	0.02	< 0.1
Ren. and fact. scales	0.02	0.1	0.02	0.01	< 0.1
ME/PS matching	− 0.08 ± 0.09	+ 0.1	+ 0.03 ± 0.05	− 0.05 ± 0.07	+ 0.1
ME generator	+ 0.15 ± 0.23	+ 0.2	+ 0.32 ± 0.14	+ 0.20 ± 0.19	+ 0.1
ISR PS scale	+ 0.07 ± 0.09	+ 0.1	+ 0.10 ± 0.05	+ 0.06 ± 0.07	< 0.1
FSR PS scale	+ 0.24 ± 0.06	− 0.4	− 0.22 ± 0.04	+ 0.13 ± 0.05	− 0.3
Top quark p_T	+ 0.02	− 0.1	− 0.06	− 0.01	− 0.1
Underlying event	− 0.10 ± 0.08	+ 0.1	+ 0.01 ± 0.05	− 0.07 ± 0.07	+ 0.1
Early resonance decays	− 0.22 ± 0.09	+ 0.8	+ 0.42 ± 0.05	− 0.03 ± 0.07	+ 0.5
Color reconnection	+ 0.34 ± 0.09	− 0.1	+ 0.23 ± 0.06	+ 0.31 ± 0.08	− 0.1
Total systematic	**0.75**	**1.1**	**1.10**	**0.62**	**0.8**
Statistical (expected)	0.09	0.1	0.06	0.08	0.1
Total (expected)	**0.76**	**1.1**	**1.10**	**0.63**	**0.8**

mination of m_t and JSF, i.e., the m_t^{fit} observable is affected differently from m_W^{reco}. For the hybrid analysis, a hybrid weight of $w_{hyb} = 0.3$ is found optimal based on the total uncertainty in the 2D result of the JSF and the jet energy scale uncertainty in the JECs. Due to the larger jet energy uncertainties at the beginning of the 13 TeV data taking, w_{hyb} is lower than in the Run 1 analysis [6] where the prior JSF knowledge contributes 50% of the information. With an expected statistical uncertainty $\delta JSF_{stat}^{2D} = 0.08\%$ on the JSF for the 2D analysis, the width of the prior is $\sigma_{prior} = 0.12\%$. The hybrid analysis leads to further reduced uncertainties in the FSR PS scale and in ERDs compared to the 2D analysis. This stems from the opposite signs of the observed shifts in m_t for the 1D and 2D analyses, i.e., the JSF from the 2D analysis overcompensates the effects on m_t^{fit}.

6 Results

The 2D fit to the selected lepton+jets events yields:

$$m_t^{2D} = 172.40 \pm 0.09 \, (\text{stat+JSF}) \pm 0.75 \, (\text{syst}) \, \text{GeV},$$
$$\text{JSF}^{2D} = 0.994 \pm 0.001 \, (\text{stat}) \pm 0.011 \, (\text{syst}).$$

As the top quark mass and the JSF are measured simultaneously, the statistical uncertainty in m_t originates from both quantities of interest. The measured unconstrained JSF is compatible with the one obtained from jets recoiling against photons and Z bosons within its uncertainties.

Separate fits to the 101 992 muon+jets events and the 59 504 electron+jets events give statistically compatible results:

$$\mu + \text{jets}: m_t^{2D} = 172.44 \pm 0.11 \, (\text{stat+JSF}) \, \text{GeV},$$
$$\text{JSF}^{2D} = 0.995 \pm 0.001 \, (\text{stat}),$$
$$\text{e} + \text{jets}: m_t^{2D} = 172.32 \pm 0.16 \, (\text{stat+JSF}) \, \text{GeV},$$
$$\text{JSF}^{2D} = 0.993 \pm 0.001 \, (\text{stat}).$$

The 1D fit and the hybrid fit with $w_{\text{hyb}} = 0.3$, as obtained in Sect. 5, yield for the lepton+jets channel:

$$m_t^{1D} = 171.93 \pm 0.06 \, (\text{stat}) \pm 1.10 \, (\text{syst}) \, \text{GeV},$$
$$m_t^{\text{hyb}} = 172.25 \pm 0.08 \, (\text{stat+JSF}) \pm 0.62 \, (\text{syst}) \, \text{GeV},$$
$$\text{JSF}^{\text{hyb}} = 0.996 \pm 0.001 \, (\text{stat}) \pm 0.008 \, (\text{syst}).$$

The hybrid fit measurement of $m_t = 172.25 \pm 0.08$ (stat+JSF) ± 0.62 (syst) GeV offers the lowest overall uncertainty and, therefore, is chosen as the main result of this study. This is the first published result of the top quark mass measured with Run 2 data and the new NLO generator setups. Because of the larger integrated luminosity and the higher $t\bar{t}$ cross section at $\sqrt{s} = 13$ TeV, the statistical uncertainty is halved compared to the Run 1 result of $m_t = 172.35 \pm 0.16$ (stat+JSF) ± 0.48 (syst) GeV [6]. This measurement is consistent with the Run 1 result within the uncertainties. The previous measurement was calibrated with $t\bar{t}$ events generated at LO with MADGRAPH 5.1.5.11 [71] matched to PYTHIA 6.426 PS [56] with the Z2* tune [72] using the MLM prescription. No shift in the measured top quark mass from the new simulation at NLO with POWHEG v2 and PYTHIA 8 and the new experimental setup is observed. The systematic uncertainties are larger than for the Run 1 result due to a more advanced treatment of the modeling uncertainties. This is mainly caused by the evaluation of a broader set of color-reconnection models that were not available in Run 1, yielding a more extensive treatment of the associated uncertainty. Without the uncertainty due to these models of 0.31 GeV, the systematic uncertainties in m_t would be reduced from 0.62 to 0.54 GeV and would be much closer

to the Run 1 result. Tighter constraints on the existing color-reconnection models and the settings in the NLO simulations can occur in the near future and reduce the systematic uncertainties due to these specific models. The new treatment of the modeling uncertainties will require special care when combining this measurement with the Run 1 result.

7 Measured top quark mass as a function of kinematic observables

The modeling of soft and perturbative QCD effects is the main source of systematic uncertainties on the analysis presented here. Differential measurements of m_t as a function of the kinematic properties of the $t\bar{t}$ system can be used to validate the different models and to identify possible biases in the measurement. Variables are selected that probe potential effects from color reconnection, ISR and FSR, and the kinematic observables of the jets coming from the top quark decays. They are the transverse momentum of the hadronically decaying top quark ($p_T^{t,\text{had}}$), the invariant mass of the $t\bar{t}$ system ($m_{t\bar{t}}$), the transverse momentum of the $t\bar{t}$ system ($p_T^{t\bar{t}}$), the number of jets with $p_T > 30$ GeV (N_{jets}), the p_T and the pseudorapidity of the b jet assigned to the hadronic decay branch ($p_T^{b,\text{had}}$ and $|\eta^{b,\text{had}}|$), the ΔR between the b jets ($\Delta R_{b\bar{b}}$), and the ΔR between the light-quark jets ($\Delta R_{q\bar{q}'}$). These are the same variables as in the Run 1 analysis [6].

For each variable, the event sample is divided into three to five bins as a function of the value of this variable, and we populate each bin using all permutations which lie within the bin boundaries. As some variables depend on the parton-jet assignment that cannot be resolved unambiguously, such as the p_T of a reconstructed top quark, a single event is allowed to contribute to multiple bins. For each bin, m_t is measured using the hybrid likelihood fit with the same probability density functions as for the inclusive measurement. The JSF prior is chosen such that it constrains the measured JSF with the same relative strength. This procedure was also used in the Run 1 analysis [6].

For the modeling of the perturbative QCD effects, the data are compared to the MG5 P8 [FxFx] M2T4, MG5 P8 [MLM] M1, and POWHEG H++ EE5C setups. For the modeling of color reconnection, the default tune of PYTHIA 8, the "QCD inspired" model [48], and the "gluon move" model [47] are considered. The three latter models are simulated with ERDs in PYTHIA 8.

In these comparisons, the mean value of the measured top quark mass is subtracted from the measurement in each bin of the sample and the results are expressed in the form of offsets $m_t - \langle m_t \rangle$, where the mean comes from the inclusive measurement on the specific sample. The subtracted offsets with respect to POWHEG P8 M2T4 can be found in the Tables 1

Table 4 Compatibility of different models with the differential measurement of the top quark mass. For each variable and model, the probability of the cumulative χ^2 is computed. The setup with POWHEG v2 + HERWIG++ does not use ME corrections to the top quark decay and shows large deviations from the data

Model	χ^2 probability							
	$p_T^{t,had}$	$m_{t\bar{t}}$	$p_T^{t\bar{t}}$	N_{jets}	$p_T^{b,had}$	$|\eta^{b,had}|$	$\Delta R_{b\bar{b}}$	$\Delta R_{q\bar{q}'}$
POWHEG P8 M2T4	0.68	0.94	0.91	0.71	0.98	0.60	0.61	0.70
MG5 P8 [FxFx] M2T4	0.98	0.78	0.93	0.94	0.80	0.35	0.94	0.91
MG5 P8 [MLM] M1	0.48	0.84	0.99	0.41	0.98	0.17	0.71	0.61
POWHEG H++ EE5C	0.07	2×10^{-13}	0.52	0.72	2×10^{-4}	0.55	0.36	2×10^{-5}
POWHEG P8 ERD on	0.75	0.99	0.83	0.53	0.95	0.64	0.38	0.96
POWHEG P8 QCD inspired	0.80	0.94	0.94	0.66	0.99	0.71	0.49	0.90
POWHEG P8 gluon move	0.87	0.94	0.93	0.72	0.93	0.51	0.59	0.93

Fig. 3 Measurements of m_t as a function of the invariant mass of the $t\bar{t}$ system $m_{t\bar{t}}$ (upper left), the number of jets N_{jets} (upper right), the pseudorapidity of the b jet assigned to the hadronic decay branch $|\eta^{b,had}|$ (lower left) and the ΔR between the light-quark jets $\Delta R_{q\bar{q}'}$ (lower right) compared to different generator models The filled circles represent the data, and the other symbols are for the simulations. For reasons of clarity, the horizontal bars indicating the bin widths are shown only for the data points and each of the simulations is shown as a single offset point with a vertical error bar representing its statistical uncertainty. The statistical uncertainty of the data is displayed by the inner error bars. For the outer error bars, the systematic uncertainties are added in quadrature
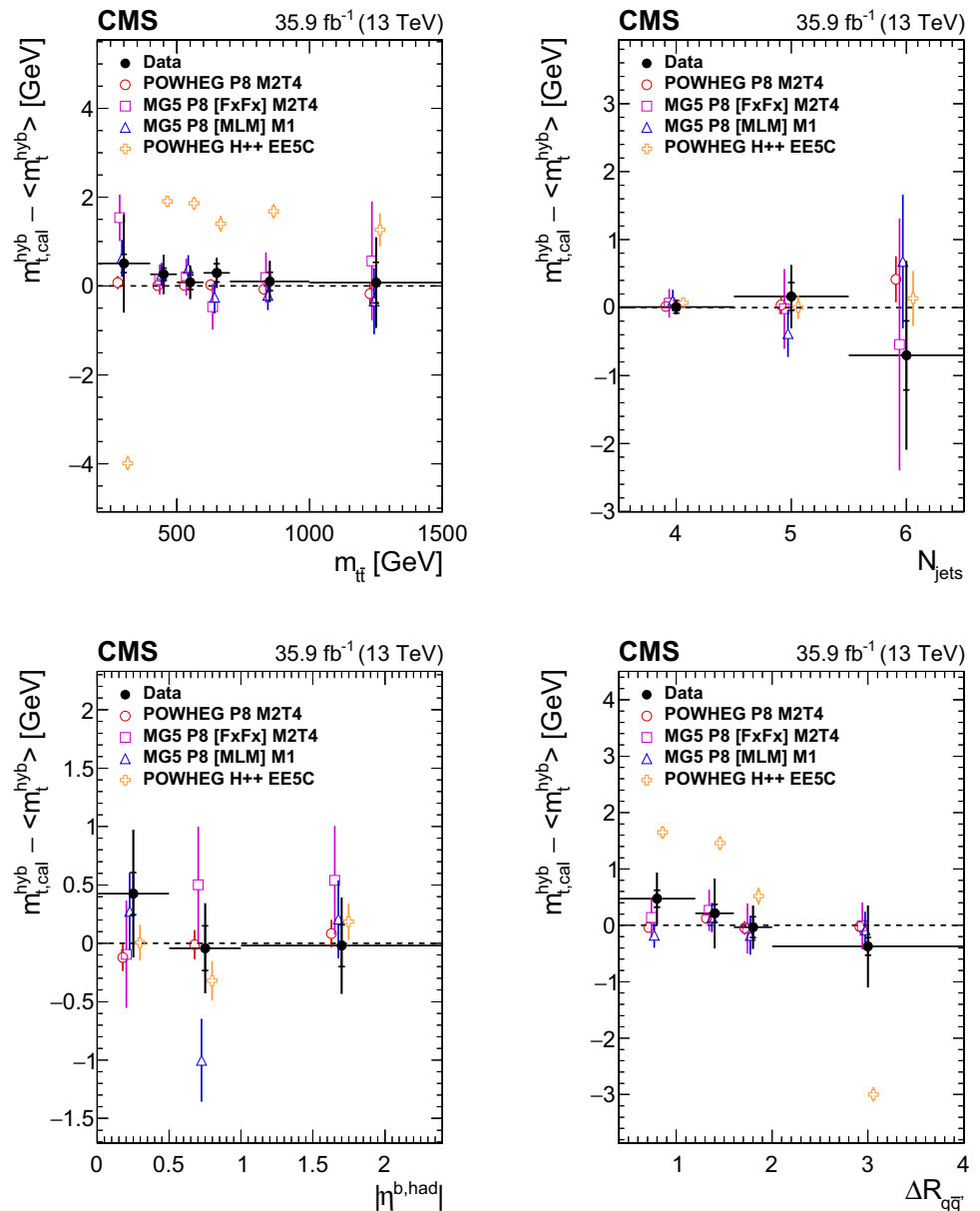
Fig. 4 Measurements of m_t as a function of the ΔR between the b jets $\Delta R_{b\bar{b}}$ (left) and the light-quark jets $\Delta R_{q\bar{q}'}$ (right) compared to alternative models of color reconnection. The symbols and conventions are the same as in Fig. 3
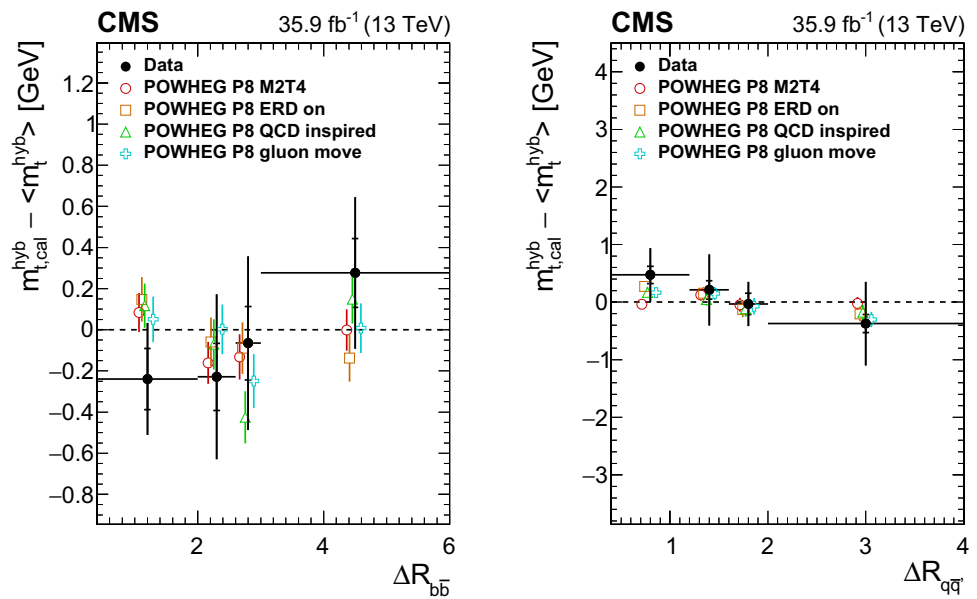
and 2. To aid in the interpretation of a difference between the value of $m_t - \langle m_t \rangle$ and the prediction from a simulation in the same bin, a bin-by-bin calibration of the results is applied. This is derived using the POWHEG P8 M2T4 simulation with the same technique as for the inclusive measurement except that it is performed for each bin separately. The bin-by-bin bias correction for the mass can be much larger than for the inclusive analysis and reaches up to 10 GeV for some bins. For each bin the statistical uncertainty and the dominant systematic uncertainties are combined in quadrature, where the latter include JEC (p_T-, η-, and flavor-dependent), JER, pileup, b fragmentation, renormalization and factorization scales, ME/PS matching, ISR/FSR PS scales, and the underlying event.

For each variable and model, the cumulative χ^2 between the model and the data is computed taking into account the statistical uncertainty in the model prediction and the total uncertainty in the data value. The number of degrees of freedom for each variable is the number of bins minus one as the mean measured top quark mass is subtracted. The resulting χ^2 probabilities (p-values) are listed in Table 4.

No significant deviation of the measured m_t is observed for the default generator setup of POWHEG P8 M2T4 and there is no evidence for a bias in the measurement. Only POWHEG H++ EE5C differs from data and all other setups for the dependence of the mass measurement on the invariant mass of the $t\bar{t}$ system, the p_T of the b jet assigned to the hadronic decay branch, and the ΔR between the light-quark jets. Figure 3 shows the results for $m_{t\bar{t}}$, N_{jets}, $|\eta^{\text{b,had}}|$ and $\Delta R_{q\bar{q}'}$ for the different generator setups for the modeling of perturbative QCD. The large deviations confirm that the POWHEG v2 + HERWIG++ setup without ME corrections to the top quark decay needs improvements to describe the data. A bias in the measurement of the top quark mass can

be spotted by a failure of the model to reproduce differential measurements. For the color-reconnection models, the $\Delta R_{b\bar{b}}$ and $\Delta R_{q\bar{q}'}$ variables should offer the best sensitivity to the modeling of the color flow. The comparison is shown in Fig. 4, but the uncertainties in the measurements are too large to rule out any of the different models.

8 Summary

This study measured the mass of the top quark using the 2016 data at $\sqrt{s} = 13$ TeV corresponding to an integrated luminosity of 35.9 fb^{-1}, and POWHEG v2 interfaced with PYTHIA 8 with the CUETP8M2T4 tune for the simulation. The top quark mass is measured to be 172.25 ± 0.08 (stat+JSF) ± 0.62 (syst) GeV from the selected lepton+jets events. The result is consistent with the CMS measurements of Run 1 of the LHC at $\sqrt{s} = 7$ and 8 TeV, with no shift observed from the new experimental setup and the use of the next-to-leading-order matrix-element generator and the new parton-shower simulation and tune. Along with the new generator setup, a more advanced treatment of the modeling uncertainties with respect to the Run 1 analysis is employed. In particular, a broader set of color-reconnection models is considered. The top quark mass has also been studied as a function of the event-level kinematic properties, and no indications of a bias in the measurements are observed.

References

1. M. Baak et al., The global electroweak fit at NNLO and prospects for the LHC and ILC. Eur. Phys. J. C **74**, 3046 (2014). https://doi.org/10.1140/epjc/s10052-014-3046-5. arXiv:1407.3792

2. G. Degrassi et al., Higgs mass and vacuum stability in the Standard Model at NNLO. JHEP **08**, 098 (2012). https://doi.org/10.1007/JHEP08(2012)098. arXiv:1205.6497

3. Particle Data Group, C. Patrignani et al., Review of particle physics. Chin. Phys. C **40**, 100001 (2016). https://doi.org/10.1088/1674-1137/40/10/100001

4. CDF and D0 Collaborations, Combination of CDF and D0 results on the mass of the top quark using up to 9.7 fb^{-1} at the Tevatron (2016). arXiv:1608.01881

5. ATLAS Collaboration, Measurement of the top quark mass in the $t\bar{t} \to$ dilepton channel from $\sqrt{s} = 8$ TeV ATLAS data. Phys. Lett. B **761**, 350 (2016). https://doi.org/10.1016/j.physletb.2016.08.042. arXiv:1606.02179

6. CMS Collaboration, Measurement of the top quark mass using proton-proton data at $\sqrt{s} = 7$ and 8 TeV. Phys. Rev. D **93**, 072004 (2016). https://doi.org/10.1103/PhysRevD.93.072004. arXiv:1509.04044

7. A.H. Hoang, I.W. Stewart, Top mass measurements from jets and the Tevatron top-quark mass. Nucl. Phys. Proc. Suppl. **185**, 220 (2008). https://doi.org/10.1016/j.nuclphysbps.2008.10.028. arXiv:0808.0222

8. S. Moch et al., High precision fundamental constants at the TeV scale (2014). arXiv:1405.4781

9. P. Marquard, A.V. Smirnov, V.A. Smirnov, M. Steinhauser, Quark mass relations to four-loop order in perturbative QCD. Phys. Rev. Lett. **114**, 142002 (2015). https://doi.org/10.1103/PhysRevLett.114.142002. arXiv:1502.01030

10. M. Beneke, P. Marquard, P. Nason, M. Steinhauser, On the ultimate uncertainty of the top quark pole mass. Phys. Lett. B **775**, 63 (2017). https://doi.org/10.1016/j.physletb.2017.10.054. arXiv:1605.03609

11. M. Butenschoen et al., Top quark mass calibration for Monte Carlo event generators. Phys. Rev. Lett. **117**, 232001 (2016). https://doi.org/10.1103/PhysRevLett.117.232001. arXiv:1608.01318

12. A.H. Hoang, C. Lepenik, M. Preisser, On the light massive flavor dependence of the large order asymptotic behavior and the ambiguity of the pole mass. JHEP **09**, 099 (2017). https://doi.org/10.1007/JHEP09(2017)099. arXiv:1706.08526

13. P. Nason, The top quark mass at the LHC. In *10th International Workshop on Top Quark Physics (TOP2017) Braga, Portugal, September 17–22, 2017* (2018). arXiv:1801.04826

14. CMS Collaboration, The CMS experiment at the CERN LHC. JINST **3**, S08004 (2008). https://doi.org/10.1088/1748-0221/3/08/S08004

15. CMS Collaboration, Particle-flow reconstruction and global event description with the CMS detector. JINST **12**, P10003 (2017). https://doi.org/10.1088/1748-0221/12/10/P10003. arXiv:1706.04965

16. M. Cacciari, G.P. Salam, Dispelling the N^3 myth for the k_t jet-finder. Phys. Lett. B **641**, 57 (2006). https://doi.org/10.1016/j.physletb.2006.08.037. arXiv:hep-ph/0512210

17. M. Cacciari, G.P. Salam, G. Soyez, The anti-k_t jet clustering algorithm. JHEP **04**, 063 (2008). https://doi.org/10.1088/1126-6708/2008/04/063. arXiv:0802.1189

18. M. Cacciari, G.P. Salam, G. Soyez, FastJet user manual. Eur. Phys. J. C **72**, 1896 (2012). https://doi.org/10.1140/epjc/s10052-012-1896-2. arXiv:1111.6097

19. M. Cacciari, G.P. Salam, Pileup subtraction using jet areas. Phys. Lett. B **659**, 119 (2008). https://doi.org/10.1016/j.physletb.2007.09.077. arXiv:0707.1378

20. CMS Collaboration, Jet energy scale and resolution in the CMS experiment in pp collisions at 8 TeV. JINST **12**, P02014 (2017). https://doi.org/10.1088/1748-0221/12/02/P02014. arXiv:1607.03663

21. CMS Collaboration, Jet algorithms performance in 13 TeV data, CMS Physics Analysis Summary CMS-PAS-JME-16-003 (2017)

22. CMS Collaboration, CMS luminosity measurements for the 2016 data taking period, CMS Physics Analysis Summary CMS-PAS-LUM-17-001 (2017)

23. P. Nason, A new method for combining NLO QCD with shower Monte Carlo algorithms. JHEP **11**, 040 (2004). https://doi.org/10.1088/1126-6708/2004/11/040. arXiv:hep-ph/0409146

24. S. Frixione, P. Nason, C. Oleari, Matching NLO QCD computations with parton shower simulations: the POWHEG method. JHEP **11**, 070 (2007). https://doi.org/10.1088/1126-6708/2007/11/070. arXiv:0709.2092

25. S. Alioli, P. Nason, C. Oleari, E. Re, A general framework for implementing NLO calculations in shower Monte Carlo programs: the POWHEG BOX. JHEP **06**, 043 (2010). https://doi.org/10.1007/JHEP06(2010)043. arXiv:1002.2581

26. J.M. Campbell, R.K. Ellis, P. Nason, E. Re, Top-pair production and decay at NLO matched with parton showers. JHEP **04**, 114 (2015). https://doi.org/10.1007/JHEP04(2015)114. arXiv:1412.1828

27. T. Sjöstrand, S. Mrenna, P. Skands, A brief introduction to PYTHIA 8.1. Comput. Phys. Commun. **178**, 852 (2008). https://doi.org/10.1016/j.cpc.2008.01.036. arXiv:0710.3820

28. P. Skands, S. Carrazza, J. Rojo, Tuning PYTHIA 8.1: the Monash 2013 tune. Eur. Phys. J. C **74**, 3024 (2014). https://doi.org/10.1140/epjc/s10052-014-3024-y. arXiv:1404.5630

29. CMS Collaboration, Investigations of the impact of the parton shower tuning in PYTHIA 8 in the modelling of $t\bar{t}$ at $\sqrt{s} = 8$ and 13 TeV, CMS Physics Analysis Summary CMS-PAS-TOP-16-021 (2016)

30. S. Alioli, P. Nason, C. Oleari, E. Re, NLO single-top production matched with shower in POWHEG: s- and t-channel contributions. JHEP **09**, 111 (2009). https://doi.org/10.1088/1126-6708/2009/09/111. arXiv:0907.4076 (Erratum: https://doi.org/10.1007/JHEP02(2010)011)

31. E. Re, Single-top Wt-channel production matched with parton showers using the POWHEG method. Eur. Phys. J. C **71**, 1547 (2011). https://doi.org/10.1140/epjc/s10052-011-1547-z. arXiv:1009.2450

32. J. Alwall et al., The automated computation of tree-level and next-to-leading order differential cross sections, and their matching to parton shower simulations. JHEP **07**, 079 (2014). https://doi.org/10.1007/JHEP07(2014)079. arXiv:1405.0301

33. J. Alwall et al., Comparative study of various algorithms for the merging of parton showers and matrix elements in hadronic collisions. Eur. Phys. J. C **53**, 473 (2008). https://doi.org/10.1140/epjc/s10052-007-0490-5. arXiv:0706.2569

34. R. Frederix, S. Frixione, Merging meets matching in MC@NLO. JHEP **12**, 061 (2012). https://doi.org/10.1007/JHEP12(2012)061. arXiv:1209.6215

35. NNPDF Collaboration, Parton distributions for the LHC Run II. JHEP **04**, 040 (2015). https://doi.org/10.1007/JHEP04(2015)040. arXiv:1410.8849

36. M. Czakon, A. Mitov, Top++: a program for the calculation of the top-pair cross-section at hadron colliders. Comput. Phys. Commun. **185**, 2930 (2014). https://doi.org/10.1016/j.cpc.2014.06.021. arXiv:1112.5675

37. Y. Li, F. Petriello, Combining QCD and electroweak corrections to dilepton production in FEWZ. Phys. Rev. D **86**, 094034 (2012). https://doi.org/10.1103/PhysRevD.86.094034. arXiv:1208.5967

38. P. Kant, HATHOR for single top-quark production: Updated predictions and uncertainty estimates for single top-quark production in hadronic collisions. Comput. Phys. Commun. **191**, 74 (2015). https://doi.org/10.1016/j.cpc.2015.02.001. arXiv:1406.4403

39. N. Kidonakis, NNLL threshold resummation for top-pair and single-top production. Phys. Part. Nucl. **45**, 714 (2014). https://doi.org/10.1134/S1063779614040091. arXiv:1210.7813

40. GEANT4 Collaboration, GEANT4—a simulation toolkit. Nucl. Instrum. Methods A **506**, 250 (2003). https://doi.org/10.1016/S0168-9002(03)01368-8

41. CMS Collaboration, Performance of CMS muon reconstruction in pp collision events at $\sqrt{s} = 7$ TeV. JINST **7**, P10002 (2012). https://doi.org/10.1088/1748-0221/7/10/P10002. arXiv:1206.4071

42. CMS Collaboration, Performance of electron reconstruction and selection with the CMS detector in proton-proton collisions at $\sqrt{s} = 8$ TeV. JINST **10**, P06005 (2015). https://doi.org/10.1088/1748-0221/10/06/P06005. arXiv:1502.02701

43. CMS Collaboration, Identification of heavy-flavour jets with the CMS detector in pp collisions at 13 TeV. JINST **13**, P05011 (2018). https://doi.org/10.1088/1748-0221/13/05/P05011. arXiv:1712.07158

44. D0 Collaboration, Direct measurement of the top quark mass at D0. Phys. Rev. D **58**, 052001 (1998). https://doi.org/10.1103/PhysRevD.58.052001. arXiv:hep-ex/9801025

45. DELPHI Collaboration, Measurement of the mass and width of the W boson in e^+e^- collisions at $\sqrt{s} = 161 – 209$ GeV. Eur. Phys. J. C **55**, 1 (2008). https://doi.org/10.1140/epjc/s10052-008-0585-7. arXiv:0803.2534

46. CMS Collaboration, Measurement of the top-quark mass in $t\bar{t}$ events with lepton+jets final states in pp collisions at $\sqrt{s} = 7$ TeV. JHEP **12**, 105 (2012). https://doi.org/10.1007/JHEP12(2012)105. arXiv:1209.2319

47. S. Argyropoulos, T. Sjöstrand, Effects of color reconnection on $t\bar{t}$ final states at the LHC. JHEP **11**, 043 (2014). https://doi.org/10.1007/JHEP11(2014)043. arXiv:1407.6653

48. J.R. Christiansen, P. Skands, String formation beyond leading colour. JHEP **08**, 003 (2015). https://doi.org/10.1007/JHEP08(2015)003. arXiv:1505.01681

49. ATLAS and CMS Collaborations, Jet energy scale uncertainty correlations between ATLAS and CMS at 8 TeV, ATL-PHYS-PUB-2015-049, CMS-PAS-JME-15-001 (2015)

50. CMS Collaboration, Measurement of the t-channel single-top-quark production cross section and of the $| V_{tb} |$ CKM matrix element in pp collisions at $\sqrt{s} = 8$ TeV. JHEP **06**, 090 (2014). https://doi.org/10.1007/JHEP06(2014)090. arXiv:1403.7366

51. CMS Collaboration, Cross section measurement of t-channel single top quark production in pp collisions at $\sqrt{s} = 13$ TeV. Phys. Lett. B **772**, 752 (2017). https://doi.org/10.1016/j.physletb.2017.07.047. arXiv:1610.00678

52. CMS Collaboration, Measurement of the production cross section of a W boson in association with two b jets in pp collisions at $\sqrt{s} = 8$ TeV. Eur. Phys. J. C **77**, 92 (2017). https://doi.org/10.1140/epjc/s10052-016-4573-z

53. CMS Collaboration, Measurements of the associated production of a Z boson and b jets in pp collisions at $\sqrt{s} = 8$ TeV. Eur. Phys. J. C **77**, 751 (2017). https://doi.org/10.1140/epjc/s10052-017-5140-y. arXiv:1611.06507

54. CMS Collaboration, Measurement of the WZ production cross section in pp collisions at $\sqrt{(s)} = 13$ TeV. Phys. Lett. B **766**, 268 (2017). https://doi.org/10.1016/j.physletb.2017.01.011. arXiv:1607.06943

55. CMS Collaboration, Measurements of the pp $\to$ ZZ production cross section and the Z $\to 4\ell$ branching fraction, and constraints on anomalous triple gauge couplings at $\sqrt{s} = 13$ TeV. Eur. Phys. J. C **78**, 165 (2018). https://doi.org/10.1140/epjc/s10052-018-5567-9. arXiv:1709.08601

56. T. Sjöstrand, S. Mrenna, P. Skands, PYTHIA 6.4 physics and manual. JHEP **05**, 026 (2006). https://doi.org/10.1088/1126-6708/2006/05/026. arXiv:hep-ph/0603175

57. M. Bähr et al., Herwig++ physics and manual. Eur. Phys. J. C **58**, 639 (2008). https://doi.org/10.1140/epjc/s10052-008-0798-9. arXiv:0803.0883

58. ALEPH Collaboration, Study of the fragmentation of b quarks into B mesons at the Z peak. Phys. Lett. B **512**, 30 (2001). https://doi.org/10.1016/S0370-2693(01)00690-6. arXiv:hep-ex/0106051

59. DELPHI Collaboration, A study of the b-quark fragmentation function with the DELPHI detector at LEP I and an averaged distribution obtained at the Z pole. Eur. Phys. J. C **71**, 1557 (2011). https://doi.org/10.1140/epjc/s10052-011-1557-x. arXiv:1102.4748

60. M.G. Bowler, e^+e^- Production of heavy quarks in the string model. Z. Phys. **11**, 169 (1981). https://doi.org/10.1007/BF01574001

61. C. Peterson, D. Schlatter, I. Schmitt, P.M. Zerwas, Scaling violations in inclusive e^+e^- annihilation spectra. Phys. Rev. D **27**, 105 (1983). https://doi.org/10.1103/PhysRevD.27.105

62. J. Rojo et al., The PDF4LHC report on PDFs and LHC data: Results from Run I and preparation for Run II. J. Phys. G **42**, 103103 (2015). https://doi.org/10.1088/0954-3899/42/10/103103. arXiv:1507.00556

63. J. Butterworth et al., PDF4LHC recommendations for LHC Run II. J. Phys. G **43**, 023001 (2016). https://doi.org/10.1088/0954-3899/43/2/023001. arXiv:1510.03865

64. A. Accardi et al., A critical appraisal and evaluation of modern PDFs. Eur. Phys. J. C **76**, 471 (2016). https://doi.org/10.1140/epjc/s10052-016-4285-4. arXiv:1603.08906

65. M. Czakon, D. Heymes, A. Mitov, High-precision differential predictions for top-quark pairs at the LHC. Phys. Rev. Lett. **116**, 082003 (2016). https://doi.org/10.1103/PhysRevLett.116.082003. arXiv:1511.00549

66. CMS Collaboration, Measurement of differential cross sections for top quark pair production using the lepton+jets final state in proton-proton collisions at 13 TeV. Phys. Rev. D **95**, 092001 (2017). https://doi.org/10.1103/PhysRevD.95.092001. arXiv:1610.04191

67. CMS Collaboration, Measurement of normalized differential $t\bar{t}$ cross sections in the dilepton channel from pp collisions at $\sqrt{s} = 13$ TeV, (2017). arXiv:1708.07638. Submitted to *JHEP*

68. CMS Collaboration, Study of the underlying event in top quark pair production in pp collisions at 13 TeV (2018). arXiv:1807.02810. Submitted to Eur. Phys. J. C

69. M.H. Seymour, A. Siodmok, Constraining MPI models using σ_{eff} and recent Tevatron and LHC underlying event data. JHEP **10**, 113 (2013). https://doi.org/10.1007/JHEP10(2013)113. arXiv:1307.5015

70. CMS Collaboration, Measurement of differential cross sections for the production of top quark pairs and of additional jets in lepton+jets events from pp collisions at $\sqrt{s} = 13$ TeV. Phys. Rev. D **97**, 112003 (2018). https://doi.org/10.1103/PhysRevD.97.112003. arXiv:1803.08856

71. J. Alwall et al., MadGraph 5: going beyond. JHEP **06**, 128 (2011). https://doi.org/10.1007/JHEP06(2011)128. arXiv:1106.0522

72. R. Field, Early LHC underlying event data—findings and surprises (2010). arXiv:1010.3558

CMS Collaboration

Yerevan Physics Institute, Yerevan, Armenia
A. M. Sirunyan, A. Tumasyan

Institut für Hochenergiephysik, Vienna, Austria
W. Adam, F. Ambrogi, E. Asilar, T. Bergauer, J. Brandstetter, E. Brondolin, M. Dragicevic, J. Erö, A. Escalante Del Valle, M. Flechl, M. Friedl, R. Frühwirth[1], V. M. Ghete, J. Hrubec, M. Jeitler[1], N. Krammer, I. Krätschmer, D. Liko, T. Madlener, I. Mikulec, N. Rad, H. Rohringer, J. Schieck[1], R. Schöfbeck, M. Spanring, D. Spitzbart, A. Taurok, W. Waltenberger, J. Wittmann, C.-E. Wulz[1], M. Zarucki

Institute for Nuclear Problems, Minsk, Belarus
V. Chekhovsky, V. Mossolov, J. Suarez Gonzalez

Universiteit Antwerpen, Antwerp, Belgium
E. A. De Wolf, D. Di Croce, X. Janssen, J. Lauwers, M. Pieters, M. Van De Klundert, H. Van Haevermaet, P. Van Mechelen, N. Van Remortel

Vrije Universiteit Brussel, Brussels, Belgium
S. Abu Zeid, F. Blekman, J. D'Hondt, I. De Bruyn, J. De Clercq, K. Deroover, G. Flouris, D. Lontkovskyi, S. Lowette, I. Marchesini, S. Moortgat, L. Moreels, Q. Python, K. Skovpen, S. Tavernier, W. Van Doninck, P. Van Mulders, I. Van Parijs

Université Libre de Bruxelles, Brussels, Belgium
D. Beghin, B. Bilin, H. Brun, B. Clerbaux, G. De Lentdecker, H. Delannoy, B. Dorney, G. Fasanella, L. Favart, R. Goldouzian, A. Grebenyuk, A. K. Kalsi, T. Lenzi, J. Luetic, T. Seva, E. Starling, C. Vander Velde, P. Vanlaer, D. Vannerom, R. Yonamine

Ghent University, Ghent, Belgium
T. Cornelis, D. Dobur, A. Fagot, M. Gul, I. Khvastunov[2], D. Poyraz, C. Roskas, D. Trocino, M. Tytgat, W. Verbeke, B. Vermassen, M. Vit, N. Zaganidis

Université Catholique de Louvain, Louvain-la-Neuve, Belgium
H. Bakhshiansohi, O. Bondu, S. Brochet, G. Bruno, C. Caputo, A. Caudron, P. David, S. De Visscher, C. Delaere, M. Delcourt, B. Francois, A. Giammanco, G. Krintiras, V. Lemaitre, A. Magitteri, A. Mertens, M. Musich, K. Piotrzkowski, L. Quertenmont, A. Saggio, M. Vidal Marono, S. Wertz, J. Zobec

Centro Brasileiro de Pesquisas Fisicas, Rio de Janeiro, Brazil
W. L. Aldá Júnior, F. L. Alves, G. A. Alves, L. Brito, G. Correia Silva, C. Hensel, A. Moraes, M. E. Pol, P. Rebello Teles

Universidade do Estado do Rio de Janeiro, Rio de Janeiro, Brazil
E. Belchior Batista Das Chagas, W. Carvalho, J. Chinellato[3], E. Coelho, E. M. Da Costa, G. G. Da Silveira[4],
D. De Jesus Damiao, S. Fonseca De Souza, H. Malbouisson, M. Medina Jaime[5], M. Melo De Almeida, C. Mora Herrera,
L. Mundim, H. Nogima, L. J. Sanchez Rosas, A. Santoro, A. Sznajder, M. Thiel, E. J. Tonelli Manganote[3],
F. Torres Da Silva De Araujo, A. Vilela Pereira

Universidade Estadual Paulista[a], Universidade Federal do ABC[b], São Paulo, Brazil
S. Ahuja[a], C. A. Bernardes[a], L. Calligaris[a], T. R. Fernandez Perez Tomei[a], E. M. Gregores[b], P. G. Mercadante[b],
S. F. Novaes[a], Sandra S. Padula[a], D. Romero Abad[b], J. C. Ruiz Vargas[a]

Institute for Nuclear Research and Nuclear Energy, Bulgarian Academy of Sciences, Sofia, Bulgaria
A. Aleksandrov, R. Hadjiiska, P. Iaydjiev, A. Marinov, M. Misheva, M. Rodozov, M. Shopova, G. Sultanov

University of Sofia, Sofia, Bulgaria
A. Dimitrov, L. Litov, B. Pavlov, P. Petkov

Beihang University, Beijing, China
W. Fang[6], X. Gao[6], L. Yuan

Institute of High Energy Physics, Beijing, China
M. Ahmad, J. G. Bian, G. M. Chen, H. S. Chen, M. Chen, Y. Chen, C. H. Jiang, D. Leggat, H. Liao, Z. Liu, F. Romeo,
S. M. Shaheen, A. Spiezia, J. Tao, C. Wang, Z. Wang, E. Yazgan, H. Zhang, J. Zhao

State Key Laboratory of Nuclear Physics and Technology, Peking University, Beijing, China
Y. Ban, G. Chen, J. Li, Q. Li, S. Liu, Y. Mao, S. J. Qian, D. Wang, Z. Xu

Tsinghua University, Beijing, China
Y. Wang

Universidad de Los Andes, Bogota, Colombia
C. Avila, A. Cabrera, C. A. Carrillo Montoya, L. F. Chaparro Sierra, C. Florez, C. F. González Hernández,
M. A. Segura Delgado

University of Split, Faculty of Electrical Engineering, Mechanical Engineering and Naval Architecture, Split, Croatia
B. Courbon, N. Godinovic, D. Lelas, I. Puljak, T. Sculac

University of Split, Faculty of Science, Split, Croatia
Z. Antunovic, M. Kovac

Institute Rudjer Boskovic, Zagreb, Croatia
V. Brigljevic, D. Ferencek, K. Kadija, B. Mesic, A. Starodumov[7], T. Susa

University of Cyprus, Nicosia, Cyprus
M. W. Ather, A. Attikis, G. Mavromanolakis, J. Mousa, C. Nicolaou, F. Ptochos, P. A. Razis, H. Rykaczewski

Charles University, Prague, Czech Republic
M. Finger[8], M. Finger Jr.[8]

Universidad San Francisco de Quito, Quito, Ecuador
E. Carrera Jarrin

Academy of Scientific Research and Technology of the Arab Republic of Egypt, Egyptian Network of High Energy Physics, Cairo, Egypt
M. A. Mahmoud[9,10], Elgammal A. Mohamed[11], E. Salama[10,12]

National Institute of Chemical Physics and Biophysics, Tallinn, Estonia
S. Bhowmik, R. K. Dewanjee, M. Kadastik, L. Perrini, M. Raidal, C. Veelken

Department of Physics, University of Helsinki, Helsinki, Finland
P. Eerola, H. Kirschenmann, J. Pekkanen, M. Voutilainen

Helsinki Institute of Physics, Helsinki, Finland
J. Havukainen, J. K. Heikkilä, T. Järvinen, V. Karimäki, R. Kinnunen, T. Lampén, K. Lassila-Perini, S. Laurila, S. Lehti,
T. Lindén, P. Luukka, T. Mäenpää, H. Siikonen, E. Tuominen, J. Tuominiemi

Lappeenranta University of Technology, Lappeenranta, Finland
T. Tuuva

IRFU, CEA, Université Paris-Saclay, Gif-sur-Yvette, France
M. Besancon, F. Couderc, M. Dejardin, D. Denegri, J. L. Faure, F. Ferri, S. Ganjour, S. Ghosh[13], A. Givernaud, P. Gras,
G. Hamel de Monchenault, P. Jarry, C. Leloup, E. Locci, M. Machet, J. Malcles, G. Negro, J. Rander, A. Rosowsky,
M. Ö. Sahin, M. Titov

Laboratoire Leprince-Ringuet, Ecole polytechnique, CNRS/IN2P3, Université Paris-Saclay, Palaiseau, France
A. Abdulsalam[14], C. Amendola, I. Antropov, S. Baffioni, F. Beaudette, P. Busson, L. Cadamuro, C. Charlot,
R. Granier de Cassagnac, M. Jo, I. Kucher, S. Lisniak, A. Lobanov, J. Martin Blanco, M. Nguyen, C. Ochando, G. Ortona,
P. Paganini, P. Pigard, R. Salerno, J. B. Sauvan, Y. Sirois, A. G. Stahl Leiton, Y. Yilmaz, A. Zabi, A. Zghiche

Université de Strasbourg, CNRS, IPHC UMR 7178, 67000 Strasbourg, France
J.-L. Agram[15], J. Andrea, D. Bloch, J.-M. Brom, E. C. Chabert, C. Collard, E. Conte[15], X. Coubez, F. Drouhin[15],
J.-C. Fontaine[15], D. Gelé, U. Goerlach, M. Jansová, P. Juillot, A.-C. Le Bihan, N. Tonon, P. Van Hove

Centre de Calcul de l'Institut National de Physique Nucleaire et de Physique des Particules, CNRS/IN2P3, Villeurbanne, France
S. Gadrat

Université de Lyon, Université Claude Bernard Lyon 1, CNRS-IN2P3, Institut de Physique Nucléaire de Lyon, Villeurbanne, France
S. Beauceron, C. Bernet, G. Boudoul, N. Chanon, R. Chierici, D. Contardo, P. Depasse, H. El Mamouni, J. Fay, L. Finco,
S. Gascon, M. Gouzevitch, G. Grenier, B. Ille, F. Lagarde, I. B. Laktineh, H. Lattaud, M. Lethuillier, L. Mirabito,
A. L. Pequegnot, S. Perries, A. Popov[16], V. Sordini, M. Vander Donckt, S. Viret, S. Zhang

Georgian Technical University, Tbilisi, Georgia
T. Toriashvili[17]

Tbilisi State University, Tbilisi, Georgia
Z. Tsamalaidze[8]

RWTH Aachen University, I. Physikalisches Institut, Aachen, Germany
C. Autermann, L. Feld, M. K. Kiesel, K. Klein, M. Lipinski, M. Preuten, M. P. Rauch, C. Schomakers, J. Schulz,
M. Teroerde, B. Wittmer, V. Zhukov[16]

RWTH Aachen University, III. Physikalisches Institut A, Aachen, Germany
A. Albert, D. Duchardt, M. Endres, M. Erdmann, S. Erdweg, T. Esch, R. Fischer, A. Güth, T. Hebbeker, C. Heidemann,
K. Hoepfner, S. Knutzen, M. Merschmeyer, A. Meyer, P. Millet, S. Mukherjee, T. Pook, M. Radziej, H. Reithler,
M. Rieger, F. Scheuch, D. Teyssier, S. Thüer

RWTH Aachen University, III. Physikalisches Institut B, Aachen, Germany
G. Flügge, B. Kargoll, T. Kress, A. Künsken, T. Müller, A. Nehrkorn, A. Nowack, C. Pistone, O. Pooth, A. Stahl[18]

Deutsches Elektronen-Synchrotron, Hamburg, Germany
M. Aldaya Martin, T. Arndt, C. Asawatangtrakuldee, I. Babounikau, K. Beernaert, O. Behnke, U. Behrens,
A. Bermúdez Martínez, D. Bertsche, A. A. Bin Anuar, K. Borras[13], V. Botta, A. Campbell, P. Connor,
C. Contreras-Campana, F. Costanza, V. Danilov, A. De Wit, C. Diez Pardos, D. Domínguez Damiani, G. Eckerlin,
D. Eckstein, T. Eichhorn, A. Elwood, E. Eren, E. Gallo[19], J. Garay Garcia, A. Geiser, J. M. Grados Luyando,
A. Grohsjean, P. Gunnellini, M. Guthoff, A. Harb, J. Hauk, H. Jung, M. Kasemann, J. Keaveney, C. Kleinwort, J. Knolle,
I. Korol, D. Krücker, W. Lange, A. Lelek, T. Lenz, K. Lipka, W. Lohmann[20], R. Mankel, I.-A. Melzer-Pellmann,

A. B. Meyer, M. Meyer, M. Missiroli, G. Mittag, J. Mnich, A. Mussgiller, S. K. Pflitsch, D. Pitzl, A. Raspereza, M. Savitskyi, P. Saxena, C. Schwanenberger, R. Shevchenko, A. Singh, N. Stefaniuk, H. Tholen, G. P. Van Onsem, R. Walsh, Y. Wen, K. Wichmann, C. Wissing, O. Zenaiev

University of Hamburg, Hamburg, Germany
R. Aggleton, S. Bein, V. Blobel, M. Centis Vignali, T. Dreyer, C. Garbers, E. Garutti, D. Gonzalez, J. Haller, A. Hinzmann, M. Hoffmann, A. Karavdina, G. Kasieczka, R. Klanner, R. Kogler, N. Kovalchuk, S. Kurz, V. Kutzner, J. Lange, D. Marconi, J. Multhaup, M. Niedziela, D. Nowatschin, T. Peiffer, A. Perieanu, A. Reimers, C. Scharf, P. Schleper, A. Schmidt, S. Schumann, J. Schwandt, J. Sonneveld, H. Stadie, G. Steinbrück, F. M. Stober, M. Stöver, D. Troendle, E. Usai, A. Vanhoefer, B. Vormwald

Institut für Experimentelle Teilchenphysik, Karlsruhe, Germany
M. Akbiyik, C. Barth, M. Baselga, S. Baur, E. Butz, R. Caspart, T. Chwalek, F. Colombo, W. De Boer, A. Dierlamm, N. Faltermann, B. Freund, R. Friese, M. Giffels, M. A. Harrendorf, F. Hartmann[18], S. M. Heindl, U. Husemann, F. Kassel[18], S. Kudella, H. Mildner, M. U. Mozer, Th. Müller, M. Plagge, G. Quast, K. Rabbertz, M. Schröder, I. Shvetsov, G. Sieber, H. J. Simonis, R. Ulrich, S. Wayand, M. Weber, T. Weiler, S. Williamson, C. Wöhrmann, R. Wolf

Institute of Nuclear and Particle Physics (INPP), NCSR Demokritos, Aghia Paraskevi, Greece
G. Anagnostou, G. Daskalakis, T. Geralis, A. Kyriakis, D. Loukas, I. Topsis-Giotis

National and Kapodistrian University of Athens, Athens, Greece
G. Karathanasis, S. Kesisoglou, A. Panagiotou, N. Saoulidou, E. Tziaferi

National Technical University of Athens, Athens, Greece
K. Kousouris, I. Papakrivopoulos

University of Ioánnina, Ioánnina, Greece
I. Evangelou, C. Foudas, P. Gianneios, P. Katsoulis, P. Kokkas, S. Mallios, N. Manthos, I. Papadopoulos, E. Paradas, J. Strologas, F. A. Triantis, D. Tsitsonis

MTA-ELTE Lendület CMS Particle and Nuclear Physics Group, Eötvös Loránd University, Budapest, Hungary
M. Csanad, N. Filipovic, G. Pasztor, O. Surányi, G. I. Veres

Wigner Research Centre for Physics, Budapest, Hungary
G. Bencze, C. Hajdu, D. Horvath[21], Á. Hunyadi, F. Sikler, T. Á. Vámi, V. Veszpremi, G. Vesztergombi[†]

Institute of Nuclear Research ATOMKI, Debrecen, Hungary
N. Beni, S. Czellar, J. Karancsi[23], A. Makovec, J. Molnar, Z. Szillasi

Institute of Physics, University of Debrecen, Debrecen, Hungary
M. Bartók[22], P. Raics, Z. L. Trocsanyi, B. Ujvari

Indian Institute of Science (IISc), Bangalore, India
S. Choudhury, J. R. Komaragiri

National Institute of Science Education and Research, Bhubaneswar, India
S. Bahinipati[24], P. Mal, K. Mandal, A. Nayak[25], D. K. Sahoo[24], S. K. Swain

Panjab University, Chandigarh, India
S. Bansal, S. B. Beri, V. Bhatnagar, S. Chauhan, R. Chawla, N. Dhingra, R. Gupta, A. Kaur, M. Kaur, S. Kaur, R. Kumar, P. Kumari, M. Lohan, A. Mehta, S. Sharma, J. B. Singh, G. Walia

University of Delhi, Delhi, India
A. Bhardwaj, B. C. Choudhary, R. B. Garg, S. Keshri, A. Kumar, Ashok Kumar, S. Malhotra, M. Naimuddin, K. Ranjan, Aashaq Shah, R. Sharma

Saha Institute of Nuclear Physics, HBNI, Kolkata, India

R. Bhardwaj[26], R. Bhattacharya, S. Bhattacharya, U. Bhawandeep[26], D. Bhowmik, S. Dey, S. Dutt[26], S. Dutta, S. Ghosh, N. Majumdar, K. Mondal, S. Mukhopadhyay, S. Nandan, A. Purohit, P. K. Rout, A. Roy, S. Roy Chowdhury, S. Sarkar, M. Sharan, B. Singh, S. Thakur[26]

Indian Institute of Technology Madras, Madras, India

P. K. Behera

Bhabha Atomic Research Centre, Mumbai, India

R. Chudasama, D. Dutta, V. Jha, V. Kumar, A. K. Mohanty[18], P. K. Netrakanti, L. M. Pant, P. Shukla, A. Topkar

Tata Institute of Fundamental Research-A, Mumbai, India

T. Aziz, S. Dugad, B. Mahakud, S. Mitra, G. B. Mohanty, N. Sur, B. Sutar

Tata Institute of Fundamental Research-B, Mumbai, India

S. Banerjee, S. Bhattacharya, S. Chatterjee, P. Das, M. Guchait, Sa. Jain, S. Kumar, M. Maity[27], G. Majumder, K. Mazumdar, N. Sahoo, T. Sarkar[27], N. Wickramage[28]

Indian Institute of Science Education and Research (IISER), Pune, India

S. Chauhan, S. Dube, V. Hegde, A. Kapoor, K. Kothekar, S. Pandey, A. Rane, S. Sharma

Institute for Research in Fundamental Sciences (IPM), Tehran, Iran

S. Chenarani[29], E. Eskandari Tadavani, S. M. Etesami[29], M. Khakzad, M. Mohammadi Najafabadi, M. Naseri, S. Paktinat Mehdiabadi[30], F. Rezaei Hosseinabadi, B. Safarzadeh[31], M. Zeinali

University College Dublin, Dublin, Ireland

M. Felcini, M. Grunewald

INFN Sezione di Bari[a]**, Università di Bari**[b]**, Politecnico di Bari**[c]**, Bari, Italy**

M. Abbrescia[a,b], C. Calabria[a,b], A. Colaleo[a], D. Creanza[a,c], L. Cristella[a,b], N. De Filippis[a,c], M. De Palma[a,b], A. Di Florio[a,b], F. Errico[a,b], L. Fiore[a], A. Gelmi[a,b], G. Iaselli[a,c], S. Lezki[a,b], G. Maggi[a,c], M. Maggi[a], B. Marangelli[a,b], G. Miniello[a,b], S. My[a,b], S. Nuzzo[a,b], A. Pompili[a,b], G. Pugliese[a,c], R. Radogna[a], A. Ranieri[a], G. Selvaggi[a,b], A. Sharma[a], L. Silvestris[a,18], R. Venditti[a], P. Verwilligen[a], G. Zito[a]

INFN Sezione di Bologna[a]**, Università di Bologna**[b]**, Bologna, Italy**

G. Abbiendi[a], C. Battilana[a,b], D. Bonacorsi[a,b], L. Borgonovi[a,b], S. Braibant-Giacomelli[a,b], L. Brigliadori[a,b], R. Campanini[a,b], P. Capiluppi[a,b], A. Castro[a,b], F. R. Cavallo[a], S. S. Chhibra[a,b], G. Codispoti[a,b], M. Cuffiani[a,b], G. M. Dallavalle[a], F. Fabbri[a], A. Fanfani[a,b], D. Fasanella[a,b], P. Giacomelli[a], C. Grandi[a], L. Guiducci[a,b], F. Iemmi, S. Marcellini[a], G. Masetti[a], A. Montanari[a], F. L. Navarria[a,b], A. Perrotta[a], T. Rovelli[a,b], G. P. Siroli[a,b], N. Tosi[a]

INFN Sezione di Catania[a]**, Università di Catania**[b]**, Catania, Italy**

S. Albergo[a,b], S. Costa[a,b], A. Di Mattia[a], F. Giordano[a,b], R. Potenza[a,b], A. Tricomi[a,b], C. Tuve[a,b]

INFN Sezione di Firenze[a]**, Università di Firenze**[b]**, Florence, Italy**

G. Barbagli[a], K. Chatterjee[a,b], V. Ciulli[a,b], C. Civinini[a], R. D'Alessandro[a,b], E. Focardi[a,b], G. Latino, P. Lenzi[a,b], M. Meschini[a], S. Paoletti[a], L. Russo[a,32], G. Sguazzoni[a], D. Strom[a], L. Viliani[a]

INFN Laboratori Nazionali di Frascati, Frascati, Italy

L. Benussi, S. Bianco, F. Fabbri, D. Piccolo, F. Primavera[18]

INFN Sezione di Genova[a]**, Università di Genova**[b]**, Genoa, Italy**

V. Calvelli[a,b], F. Ferro[a], F. Ravera[a,b], E. Robutti[a], S. Tosi[a,b]

INFN Sezione di Milano-Bicocca[a]**, Università di Milano-Bicocca**[b]**, Milan, Italy**

A. Benaglia[a], A. Beschi[b], L. Brianza[a,b], F. Brivio[a,b], V. Ciriolo[a,b,18], M. E. Dinardo[a,b], S. Fiorendi[a,b], S. Gennai[a], A. Ghezzi[a,b], P. Govoni[a,b], M. Malberti[a,b], S. Malvezzi[a], R. A. Manzoni[a,b], D. Menasce[a], L. Moroni[a], M. Paganoni[a,b], K. Pauwels[a,b], D. Pedrini[a], S. Pigazzini[a,b,33], S. Ragazzi[a,b], T. Tabarelli de Fatis[a,b]

INFN Sezione di Napoli[a]**, Università di Napoli 'Federico II'** [b]**, Naples, Italy, Università della Basilicata**[c]**, Potenza, Italy, Università G. Marconi**[d]**, Rome, Italy**

S. Buontempo^a, N. Cavallo^{a,c}, S. Di Guida^{a,d,18}, F. Fabozzi^{a,c}, F. Fienga^{a,b}, G. Galati^{a,b}, A. O. M. Iorio^{a,b}, W. A. Khan^a, L. Lista^a, S. Meola^{a,d,18}, P. Paolucci^{a,18}, C. Sciacca^{a,b}, F. Thyssen^a, E. Voevodina^{a,b}

INFN Sezione di Padova^a, Università di Padova^b, Padua, Italy, Università di Trento^c, Trento, Italy
P. Azzi^a, N. Bacchetta^a, L. Benato^{a,b}, D. Bisello^{a,b}, A. Boletti^{a,b}, R. Carlin^{a,b}, P. Checchia^a, M. Dall'Osso^{a,b}, P. De Castro Manzano^a, T. Dorigo^a, U. Dosselli^a, F. Gasparini^{a,b}, U. Gasparini^{a,b}, A. Gozzelino^a, S. Lacaprara^a, P. Lujan, M. Margoni^{a,b}, A. T. Meneguzzo^{a,b}, N. Pozzobon^{a,b}, P. Ronchese^{a,b}, R. Rossin^{a,b}, F. Simonetto^{a,b}, A. Tiko, E. Torassa^a, S. Ventura^a, M. Zanetti^{a,b}, P. Zotto^{a,b}

INFN Sezione di Pavia^a, Università di Pavia^b, Pavia, Italy
A. Braghieri^a, A. Magnani^a, P. Montagna^{a,b}, S. P. Ratti^{a,b}, V. Re^a, M. Ressegotti^{a,b}, C. Riccardi^{a,b}, P. Salvini^a, I. Vai^{a,b}, P. Vitulo^{a,b}

INFN Sezione di Perugia^a, Università di Perugia^b, Perugia, Italy
L. Alunni Solestizi^{a,b}, M. Biasini^{a,b}, G. M. Bilei^a, C. Cecchi^{a,b}, D. Ciangottini^{a,b}, L. Fanò^{a,b}, P. Lariccia^{a,b}, R. Leonardi^{a,b}, E. Manoni^a, G. Mantovani^{a,b}, V. Mariani^{a,b}, M. Menichelli^a, A. Rossi^{a,b}, A. Santocchia^{a,b}, D. Spiga^a

INFN Sezione di Pisa^a, Università di Pisa^b, Scuola Normale Superiore di Pisa^c, Pisa, Italy
K. Androsov^a, P. Azzurri^a, G. Bagliesi^a, L. Bianchini^a, T. Boccali^a, L. Borrello, R. Castaldi^a, M. A. Ciocci^{a,b}, R. Dell'Orso^a, G. Fedi^a, L. Giannini^{a,c}, A. Giassi^a, M. T. Grippo^a, F. Ligabue^{a,c}, T. Lomtadze^a, E. Manca^{a,c}, G. Mandorli^{a,c}, A. Messineo^{a,b}, F. Palla^a, A. Rizzi^{a,b}, P. Spagnolo^a, R. Tenchini^a, G. Tonelli^{a,b}, A. Venturi^a, P. G. Verdini^a

INFN Sezione di Roma^a, Sapienza Università di Roma^b, Rome, Italy
L. Barone^{a,b}, F. Cavallari^a, M. Cipriani^{a,b}, N. Daci^a, D. Del Re^{a,b}, E. Di Marco^{a,b}, M. Diemoz^a, S. Gelli^{a,b}, E. Longo^{a,b}, B. Marzocchi^{a,b}, P. Meridiani^a, G. Organtini^{a,b}, F. Pandolfi^a, R. Paramatti^{a,b}, F. Preiato^{a,b}, S. Rahatlou^{a,b}, C. Rovelli^a, F. Santanastasio^{a,b}

INFN Sezione di Torino^a, Università di Torino^b, Torino, Italy, Università del Piemonte Orientale^c, Novara, Italy
N. Amapane^{a,b}, R. Arcidiacono^{a,c}, S. Argiro^{a,b}, M. Arneodo^{a,c}, N. Bartosik^a, R. Bellan^{a,b}, C. Biino^a, N. Cartiglia^a, R. Castello^{a,b}, F. Cenna^{a,b}, M. Costa^{a,b}, R. Covarelli^{a,b}, A. Degano^{a,b}, N. Demaria^a, B. Kiani^{a,b}, C. Mariotti^a, S. Maselli^a, E. Migliore^{a,b}, V. Monaco^{a,b}, E. Monteil^{a,b}, M. Monteno^a, M. M. Obertino^{a,b}, L. Pacher^{a,b}, N. Pastrone^a, M. Pelliccioni^a, G. L. Pinna Angioni^{a,b}, A. Romero^{a,b}, M. Ruspa^{a,c}, R. Sacchi^{a,b}, K. Shchelina^{a,b}, V. Sola^a, A. Solano^{a,b}, A. Staiano^a

INFN Sezione di Trieste^a, Università di Trieste^b, Trieste, Italy
S. Belforte^a, V. Candelise^{a,b}, M. Casarsa^a, F. Cossutti^a, G. Della Ricca^{a,b}, F. Vazzoler^{a,b}, A. Zanetti^a

Kyungpook National University, Daegu, Korea
D. H. Kim, G. N. Kim, M. S. Kim, J. Lee, S. Lee, S. W. Lee, C. S. Moon, Y. D. Oh, S. Sekmen, D. C. Son, Y. C. Yang

Institute for Universe and Elementary Particles, Chonnam National University, Kwangju, Korea
H. Kim, D. H. Moon, G. Oh

Hanyang University, Seoul, Korea
J. A. Brochero Cifuentes, J. Goh, T. J. Kim

Korea University, Seoul, Korea
S. Cho, S. Choi, Y. Go, D. Gyun, S. Ha, B. Hong, Y. Jo, Y. Kim, K. Lee, K. S. Lee, S. Lee, J. Lim, S. K. Park, Y. Roh

Seoul National University, Seoul, Korea
J. Almond, J. Kim, J. S. Kim, H. Lee, K. Lee, K. Nam, S. B. Oh, B. C. Radburn-Smith, S. h. Seo, U. K. Yang, H. D. Yoo, G. B. Yu

University of Seoul, Seoul, Korea
H. Kim, J. H. Kim, J. S. H. Lee, I. C. Park

Sungkyunkwan University, Suwon, Korea
Y. Choi, C. Hwang, J. Lee, I. Yu

Vilnius University, Vilnius, Lithuania
V. Dudenas, A. Juodagalvis, J. Vaitkus

National Centre for Particle Physics, Universiti Malaya, Kuala Lumpur, Malaysia
I. Ahmed, Z. A. Ibrahim, M. A. B. Md Ali[34], F. Mohamad Idris[35], W. A. T. Wan Abdullah, M. N. Yusli, Z. Zolkapli

Centro de Investigacion y de Estudios Avanzados del IPN, Mexico City, Mexico
M. C. Duran-Osuna, H. Castilla-Valdez, E. De La Cruz-Burelo, G. Ramirez-Sanchez, I. Heredia-De La Cruz[36],
R. I. Rabadan-Trejo, R. Lopez-Fernandez, J. Mejia Guisao, R. Reyes-Almanza, A. Sanchez-Hernandez

Universidad Iberoamericana, Mexico City, Mexico
S. Carrillo Moreno, C. Oropeza Barrera, F. Vazquez Valencia

Benemerita Universidad Autonoma de Puebla, Puebla, Mexico
J. Eysermans, I. Pedraza, H. A. Salazar Ibarguen, C. Uribe Estrada

Universidad Autónoma de San Luis Potosí, San Luis Potosí, Mexico
A. Morelos Pineda

University of Auckland, Auckland, New Zealand
D. Krofcheck

University of Canterbury, Christchurch, New Zealand
S. Bheesette, P. H. Butler

National Centre for Physics, Quaid-I-Azam University, Islamabad, Pakistan
A. Ahmad, M. Ahmad, Q. Hassan, H. R. Hoorani, A. Saddique, M. A. Shah, M. Shoaib, M. Waqas

National Centre for Nuclear Research, Swierk, Poland
H. Bialkowska, M. Bluj, B. Boimska, T. Frueboes, M. Górski, M. Kazana, K. Nawrocki, M. Szleper, P. Traczyk,
P. Zalewski

Institute of Experimental Physics, Faculty of Physics, University of Warsaw, Warsaw, Poland
K. Bunkowski, A. Byszuk[37], K. Doroba, A. Kalinowski, M. Konecki, J. Krolikowski, M. Misiura, M. Olszewski,
A. Pyskir, M. Walczak

Laboratório de Instrumentação e Física Experimental de Partículas, Lisbon, Portugal
P. Bargassa, C. Beirão Da Cruz E Silva, A. Di Francesco, P. Faccioli, B. Galinhas, M. Gallinaro, J. Hollar, N. Leonardo,
L. Lloret Iglesias, M. V. Nemallapudi, J. Seixas, G. Strong, O. Toldaiev, D. Vadruccio, J. Varela

Joint Institute for Nuclear Research, Dubna, Russia
A. Baginyan, I. Golutvin, A. Kamenev, V. Karjavin, V. Korenkov, G. Kozlov, A. Lanev, A. Malakhov, V. Matveev[38,39],
V. V. Mitsyn, P. Moisenz, V. Palichik, V. Perelygin, S. Shmatov, V. Smirnov, V. Trofimov, B. S. Yuldashev[40], A. Zarubin,
V. Zhiltsov

Petersburg Nuclear Physics Institute, Gatchina (St. Petersburg), Russia
Y. Ivanov, V. Kim[41], E. Kuznetsova[42], P. Levchenko, V. Murzin, V. Oreshkin, I. Smirnov, D. Sosnov, V. Sulimov,
L. Uvarov, S. Vavilov, A. Vorobyev

Institute for Nuclear Research, Moscow, Russia
Yu. Andreev, A. Dermenev, S. Gninenko, N. Golubev, A. Karneyeu, M. Kirsanov, N. Krasnikov, A. Pashenkov, D. Tlisov,
A. Toropin

Institute for Theoretical and Experimental Physics, Moscow, Russia
V. Epshteyn, V. Gavrilov, N. Lychkovskaya, V. Popov, I. Pozdnyakov, G. Safronov, A. Spiridonov, A. Stepennov,
V. Stolin, M. Toms, E. Vlasov, A. Zhokin

Moscow Institute of Physics and Technology, Moscow, Russia
T. Aushev, A. Bylinkin[39]

National Research Nuclear University 'Moscow Engineering Physics Institute' (MEPhI), Moscow, Russia
M. Chadeeva[43], P. Parygin, D. Philippov, S. Polikarpov, E. Popova, V. Rusinov

P.N. Lebedev Physical Institute, Moscow, Russia
V. Andreev, M. Azarkin[39], I. Dremin[39], M. Kirakosyan[39], S. V. Rusakov, A. Terkulov

Skobeltsyn Institute of Nuclear Physics, Lomonosov Moscow State University, Moscow, Russia
A. Baskakov, A. Belyaev, E. Boos, V. Bunichev, M. Dubinin[44], L. Dudko, V. Klyukhin, N. Korneeva, I. Lokhtin,
I. Miagkov, S. Obraztsov, M. Perfilov, S. Petrushanko, V. Savrin, A. Snigirev

Novosibirsk State University (NSU), Novosibirsk, Russia
V. Blinov[45], D. Shtol[45], Y. Skovpen[45]

**State Research Center of Russian Federation, Institute for High Energy Physics of NRC 'Kurchatov Institute',
Protvino, Russia**
I. Azhgirey, I. Bayshev, S. Bitioukov, D. Elumakhov, A. Godizov, V. Kachanov, A. Kalinin, D. Konstantinov, P. Mandrik,
V. Petrov, R. Ryutin, A. Sobol, S. Troshin, N. Tyurin, A. Uzunian, A. Volkov

National Research Tomsk Polytechnic University, Tomsk, Russia
A. Babaev

University of Belgrade, Faculty of Physics and Vinca Institute of Nuclear Sciences, Belgrade, Serbia
P. Adzic[46], P. Cirkovic, D. Devetak, M. Dordevic, J. Milosevic

Centro de Investigaciones Energéticas Medioambientales y Tecnológicas (CIEMAT), Madrid, Spain
J. Alcaraz Maestre, A. Álvarez Fernández, I. Bachiller, M. Barrio Luna, M. Cerrada, N. Colino, B. De La Cruz,
A. Delgado Peris, C. Fernandez Bedoya, J. P. Fernández Ramos, J. Flix, M. C. Fouz, O. Gonzalez Lopez, S. Goy Lopez,
J. M. Hernandez, M. I. Josa, D. Moran, A. Pérez-Calero Yzquierdo, J. Puerta Pelayo, I. Redondo, L. Romero, M. S. Soares,
A. Triossi

Universidad Autónoma de Madrid, Madrid, Spain
C. Albajar, J. F. de Trocóniz

Universidad de Oviedo, Oviedo, Spain
J. Cuevas, C. Erice, J. Fernandez Menendez, S. Folgueras, I. Gonzalez Caballero, J. R. González Fernández,
E. Palencia Cortezon, S. Sanchez Cruz, P. Vischia, J. M. Vizan Garcia

Instituto de Física de Cantabria (IFCA), CSIC-Universidad de Cantabria, Santander, Spain
I. J. Cabrillo, A. Calderon, B. Chazin Quero, J. Duarte Campderros, M. Fernandez, P. J. Fernández Manteca,
A. García Alonso, J. Garcia-Ferrero, G. Gomez, A. Lopez Virto, J. Marco, C. Martinez Rivero, P. Martinez Ruiz del Arbol,
F. Matorras, J. Piedra Gomez, C. Prieels, T. Rodrigo, A. Ruiz-Jimeno, L. Scodellaro, N. Trevisani, I. Vila,
R. Vilar Cortabitarte

CERN, European Organization for Nuclear Research, Geneva, Switzerland
D. Abbaneo, B. Akgun, E. Auffray, P. Baillon, A. H. Ball, D. Barney, J. Bendavid, M. Bianco, A. Bocci, C. Botta,
T. Camporesi, M. Cepeda, G. Cerminara, E. Chapon, Y. Chen, D. d'Enterria, A. Dabrowski, V. Daponte, A. David,
M. De Gruttola, A. De Roeck, N. Deelen, M. Dobson, T. du Pree, M. Dünser, N. Dupont, A. Elliott-Peisert, P. Everaerts,
F. Fallavollita[47], G. Franzoni, J. Fulcher, W. Funk, D. Gigi, A. Gilbert, K. Gill, F. Glege, D. Gulhan, J. Hegeman,
V. Innocente, A. Jafari, P. Janot, O. Karacheban[20], J. Kieseler, V. Knünz, A. Kornmayer, M. Krammer[1], C. Lange,
P. Lecoq, C. Lourenço, M. T. Lucchini, L. Malgeri, M. Mannelli, A. Martelli, F. Meijers, J. A. Merlin, S. Mersi, E. Meschi,
P. Milenovic[48], F. Moortgat, M. Mulders, H. Neugebauer, J. Ngadiuba, S. Orfanelli, L. Orsini, F. Pantaleo[18], L. Pape,
E. Perez, M. Peruzzi, A. Petrilli, G. Petrucciani, A. Pfeiffer, M. Pierini, F. M. Pitters, D. Rabady, A. Racz, T. Reis,
G. Rolandi[49], M. Rovere, H. Sakulin, C. Schäfer, C. Schwick, M. Seidel, M. Selvaggi, A. Sharma, P. Silva, P. Sphicas[50],
A. Stakia, J. Steggemann, M. Stoye, M. Tosi, D. Treille, A. Tsirou, V. Veckalns[51], M. Verweij, W. D. Zeuner

Paul Scherrer Institut, Villigen, Switzerland

W. Bertl[†], L. Caminada[52], K. Deiters, W. Erdmann, R. Horisberger, Q. Ingram, H. C. Kaestli, D. Kotlinski, U. Langenegger, T. Rohe, S. A. Wiederkehr

ETH Zurich, Institute for Particle Physics and Astrophysics (IPA), Zurich, Switzerland

M. Backhaus, L. Bäni, P. Berger, B. Casal, N. Chernyavskaya, G. Dissertori, M. Dittmar, M. Donegà, C. Dorfer, C. Grab, C. Heidegger, D. Hits, J. Hoss, T. Klijnsma, W. Lustermann, M. Marionneau, M. T. Meinhard, D. Meister, F. Micheli, P. Musella, F. Nessi-Tedaldi, J. Pata, F. Pauss, G. Perrin, L. Perrozzi, M. Quittnat, M. Reichmann, D. Ruini, D. A. Sanz Becerra, M. Schönenberger, L. Shchutska, V. R. Tavolaro, K. Theofilatos, M. L. Vesterbacka Olsson, R. Wallny, D. H. Zhu

Universität Zürich, Zurich, Switzerland

T. K. Aarrestad, C. Amsler[53], D. Brzhechko, M. F. Canelli, A. De Cosa, R. Del Burgo, S. Donato, C. Galloni, T. Hreus, B. Kilminster, I. Neutelings, D. Pinna, G. Rauco, P. Robmann, D. Salerno, K. Schweiger, C. Seitz, Y. Takahashi, A. Zucchetta

National Central University, Chung-Li, Taiwan

Y. H. Chang, K. y. Cheng, T. H. Doan, Sh. Jain, R. Khurana, C. M. Kuo, W. Lin, A. Pozdnyakov, S. S. Yu

National Taiwan University (NTU), Taipei, Taiwan

P. Chang, Y. Chao, K. F. Chen, P. H. Chen, F. Fiori, W.-S. Hou, Y. Hsiung, Arun Kumar, Y. F. Liu, R.-S. Lu, E. Paganis, A. Psallidas, A. Steen, J. f. Tsai

Department of Physics, Faculty of Science, Chulalongkorn University, Bangkok, Thailand

B. Asavapibhop, K. Kovitanggoon, G. Singh, N. Srimanobhas

Physics Department, Science and Art Faculty, Çukurova University, Adana, Turkey

A. Bat, F. Boran, S. Cerci[54], S. Damarseckin, Z. S. Demiroglu, C. Dozen, I. Dumanoglu, S. Girgis, G. Gokbulut, Y. Guler, I. Hos[55], E. E. Kangal[56], O. Kara, A. Kayis Topaksu, U. Kiminsu, M. Oglakci, G. Onengut, K. Ozdemir[57], D. Sunar Cerci[54], B. Tali[54], U. G. Tok, S. Turkcapar, I. S. Zorbakir, C. Zorbilmez

Physics Department, Middle East Technical University, Ankara, Turkey

G. Karapinar[58], K. Ocalan[59], M. Yalvac, M. Zeyrek

Bogazici University, Istanbul, Turkey

I. O. Atakisi, E. Gülmez, M. Kaya[60], O. Kaya[61], S. Tekten, E. A. Yetkin[62]

Istanbul Technical University, Istanbul, Turkey

M. N. Agaras, S. Atay, A. Cakir, K. Cankocak, Y. Komurcu

Institute for Scintillation Materials of National Academy of Science of Ukraine, Kharkiv, Ukraine

B. Grynyov

National Scientific Center, Kharkov Institute of Physics and Technology, Kharkiv, Ukraine

L. Levchuk

University of Bristol, Bristol, UK

F. Ball, L. Beck, J. J. Brooke, D. Burns, E. Clement, D. Cussans, O. Davignon, H. Flacher, J. Goldstein, G. P. Heath, H. F. Heath, L. Kreczko, D. M. Newbold[63], S. Paramesvaran, T. Sakuma, S. Seif El Nasr-storey, D. Smith, V. J. Smith

Rutherford Appleton Laboratory, Didcot, UK

K. W. Bell, A. Belyaev[64], C. Brew, R. M. Brown, D. Cieri, D. J. A. Cockerill, J. A. Coughlan, K. Harder, S. Harper, J. Linacre, E. Olaiya, D. Petyt, C. H. Shepherd-Themistocleous, A. Thea, I. R. Tomalin, T. Williams, W. J. Womersley

Imperial College, London, UK

G. Auzinger, R. Bainbridge, P. Bloch, J. Borg, S. Breeze, O. Buchmuller, A. Bundock, S. Casasso, D. Colling, L. Corpe, P. Dauncey, G. Davies, M. Della Negra, R. Di Maria, Y. Haddad, G. Hall, G. Iles, T. James, M. Komm, R. Lane, C. Laner, L. Lyons, A.-M. Magnan, S. Malik, L. Mastrolorenzo, T. Matsushita, J. Nash[65], A. Nikitenko[7], V. Palladino, M. Pesaresi, A. Richards, A. Rose, E. Scott, C. Seez, A. Shtipliyski, T. Strebler, S. Summers, A. Tapper, K. Uchida, M. Vazquez Acosta[66], T. Virdee[18], N. Wardle, D. Winterbottom, J. Wright, S. C. Zenz

Brunel University, Uxbridge, UK

J. E. Cole, P. R. Hobson, A. Khan, P. Kyberd, A. Morton, I. D. Reid, L. Teodorescu, S. Zahid

Baylor University, Waco, USA

A. Borzou, K. Call, J. Dittmann, K. Hatakeyama, H. Liu, N. Pastika, C. Smith

Catholic University of America, Washington, DC, USA

R. Bartek, A. Dominguez

The University of Alabama, Tuscaloosa, USA

A. Buccilli, S. I. Cooper, C. Henderson, P. Rumerio, C. West

Boston University, Boston, USA

D. Arcaro, A. Avetisyan, T. Bose, D. Gastler, D. Rankin, C. Richardson, J. Rohlf, L. Sulak, D. Zou

Brown University, Providence, USA

G. Benelli, D. Cutts, M. Hadley, J. Hakala, U. Heintz, J. M. Hogan[67], K. H. M. Kwok, E. Laird, G. Landsberg, J. Lee,
Z. Mao, M. Narain, J. Pazzini, S. Piperov, S. Sagir, R. Syarif, D. Yu

University of California, Davis, Davis, USA

R. Band, C. Brainerd, R. Breedon, D. Burns, M. Calderon De La Barca Sanchez, M. Chertok, J. Conway, R. Conway,
P. T. Cox, R. Erbacher, C. Flores, G. Funk, W. Ko, R. Lander, C. Mclean, M. Mulhearn, D. Pellett, J. Pilot, S. Shalhout,
M. Shi, J. Smith, D. Stolp, D. Taylor, K. Tos, M. Tripathi, Z. Wang, F. Zhang

University of California, Los Angeles, USA

M. Bachtis, C. Bravo, R. Cousins, A. Dasgupta, A. Florent, J. Hauser, M. Ignatenko, N. Mccoll, S. Regnard, D. Saltzberg,
C. Schnaible, V. Valuev

University of California, Riverside, Riverside, USA

E. Bouvier, K. Burt, R. Clare, J. Ellison, J. W. Gary, S. M. A. Ghiasi Shirazi, G. Hanson, G. Karapostoli, E. Kennedy,
F. Lacroix, O. R. Long, M. Olmedo Negrete, M. I. Paneva, W. Si, L. Wang, H. Wei, S. Wimpenny, B. R. Yates

University of California, San Diego, La Jolla, USA

J. G. Branson, S. Cittolin, M. Derdzinski, R. Gerosa, D. Gilbert, B. Hashemi, A. Holzner, D. Klein, G. Kole, V. Krutelyov,
J. Letts, M. Masciovecchio, D. Olivito, S. Padhi, M. Pieri, M. Sani, V. Sharma, S. Simon, M. Tadel, A. Vartak,
S. Wasserbaech[68], J. Wood, F. Würthwein, A. Yagil, G. Zevi Della Porta

University of California, Santa Barbara - Department of Physics, Santa Barbara, USA

N. Amin, R. Bhandari, J. Bradmiller-Feld, C. Campagnari, M. Citron, A. Dishaw, V. Dutta, M. Franco Sevilla, L. Gouskos,
R. Heller, J. Incandela, A. Ovcharova, H. Qu, J. Richman, D. Stuart, I. Suarez, J. Yoo

California Institute of Technology, Pasadena, USA

D. Anderson, A. Bornheim, J. Bunn, J. M. Lawhorn, H. B. Newman, T. Q. Nguyen, C. Pena, M. Spiropulu, J. R. Vlimant,
R. Wilkinson, S. Xie, Z. Zhang, R. Y. Zhu

Carnegie Mellon University, Pittsburgh, USA

M. B. Andrews, T. Ferguson, T. Mudholkar, M. Paulini, J. Russ, M. Sun, H. Vogel, I. Vorobiev, M. Weinberg

University of Colorado Boulder, Boulder, USA

J. P. Cumalat, W. T. Ford, F. Jensen, A. Johnson, M. Krohn, S. Leontsinis, E. MacDonald, T. Mulholland, K. Stenson,
K. A. Ulmer, S. R. Wagner

Cornell University, Ithaca, USA

J. Alexander, J. Chaves, Y. Cheng, J. Chu, A. Datta, K. Mcdermott, N. Mirman, J. R. Patterson, D. Quach, A. Rinkevicius,
A. Ryd, L. Skinnari, L. Soffi, S. M. Tan, Z. Tao, J. Thom, J. Tucker, P. Wittich, M. Zientek

Fermi National Accelerator Laboratory, Batavia, USA

S. Abdullin, M. Albrow, M. Alyari, G. Apollinari, A. Apresyan, A. Apyan, S. Banerjee, L. A. T. Bauerdick, A. Beretvas,
J. Berryhill, P. C. Bhat, G. Bolla[†], K. Burkett, J. N. Butler, A. Canepa, G. B. Cerati, H. W. K. Cheung, F. Chlebana,
M. Cremonesi, J. Duarte, V. D. Elvira, J. Freeman, Z. Gecse, E. Gottschalk, L. Gray, D. Green, S. Grünendahl, O. Gutsche,

J. Hanlon, R. M. Harris, S. Hasegawa, J. Hirschauer, Z. Hu, B. Jayatilaka, S. Jindariani, M. Johnson, U. Joshi, B. Klima, M. J. Kortelainen, B. Kreis, S. Lammel, D. Lincoln, R. Lipton, M. Liu, T. Liu, R. Lopes De Sá, J. Lykken, K. Maeshima, N. Magini, J. M. Marraffino, D. Mason, P. McBride, P. Merkel, S. Mrenna, S. Nahn, V. O'Dell, K. Pedro, O. Prokofyev, G. Rakness, L. Ristori, A. Savoy-Navarro[69], B. Schneider, E. Sexton-Kennedy, A. Soha, W. J. Spalding, L. Spiegel, S. Stoynev, J. Strait, N. Strobbe, L. Taylor, S. Tkaczyk, N. V. Tran, L. Uplegger, E. W. Vaandering, C. Vernieri, M. Verzocchi, R. Vidal, M. Wang, H. A. Weber, A. Whitbeck, W. Wu

University of Florida, Gainesville, USA
D. Acosta, P. Avery, P. Bortignon, D. Bourilkov, A. Brinkerhoff, A. Carnes, M. Carver, D. Curry, R. D. Field, I. K. Furic, S. V. Gleyzer, B. M. Joshi, J. Konigsberg, A. Korytov, K. Kotov, P. Ma, K. Matchev, H. Mei, G. Mitselmakher, K. Shi, D. Sperka, N. Terentyev, L. Thomas, J. Wang, S. Wang, J. Yelton

Florida International University, Miami, USA
Y. R. Joshi, S. Linn, P. Markowitz, J. L. Rodriguez

Florida State University, Tallahassee, USA
A. Ackert, T. Adams, A. Askew, S. Hagopian, V. Hagopian, K. F. Johnson, T. Kolberg, G. Martinez, T. Perry, H. Prosper, A. Saha, A. Santra, V. Sharma, R. Yohay

Florida Institute of Technology, Melbourne, USA
M. M. Baarmand, V. Bhopatkar, S. Colafranceschi, M. Hohlmann, D. Noonan, T. Roy, F. Yumiceva

University of Illinois at Chicago (UIC), Chicago, USA
M. R. Adams, L. Apanasevich, D. Berry, R. R. Betts, R. Cavanaugh, X. Chen, S. Dittmer, O. Evdokimov, C. E. Gerber, D. A. Hangal, D. J. Hofman, K. Jung, J. Kamin, I. D. Sandoval Gonzalez, M. B. Tonjes, N. Varelas, H. Wang, Z. Wu, J. Zhang

The University of Iowa, Iowa City, USA
B. Bilki[70], W. Clarida, K. Dilsiz[71], S. Durgut, R. P. Gandrajula, M. Haytmyradov, V. Khristenko, J.-P. Merlo, H. Mermerkaya[72], A. Mestvirishvili, A. Moeller, J. Nachtman, H. Ogul[73], Y. Onel, F. Ozok[74], A. Penzo, C. Snyder, E. Tiras, J. Wetzel, K. Yi

Johns Hopkins University, Baltimore, USA
B. Blumenfeld, A. Cocoros, N. Eminizer, D. Fehling, L. Feng, A. V. Gritsan, W. T. Hung, P. Maksimovic, J. Roskes, U. Sarica, M. Swartz, M. Xiao, C. You

The University of Kansas, Lawrence, USA
A. Al-bataineh, P. Baringer, A. Bean, J. F. Benitez, S. Boren, J. Bowen, J. Castle, S. Khalil, A. Kropivnitskaya, D. Majumder, W. Mcbrayer, M. Murray, C. Rogan, C. Royon, S. Sanders, E. Schmitz, J. D. Tapia Takaki, Q. Wang

Kansas State University, Manhattan, USA
A. Ivanov, K. Kaadze, Y. Maravin, A. Modak, A. Mohammadi, L. K. Saini, N. Skhirtladze

Lawrence Livermore National Laboratory, Livermore, USA
F. Rebassoo, D. Wright

University of Maryland, College Park, USA
A. Baden, O. Baron, A. Belloni, S. C. Eno, Y. Feng, C. Ferraioli, N. J. Hadley, S. Jabeen, G. Y. Jeng, R. G. Kellogg, J. Kunkle, A. C. Mignerey, F. Ricci-Tam, Y. H. Shin, A. Skuja, S. C. Tonwar

Massachusetts Institute of Technology, Cambridge, USA

D. Abercrombie, B. Allen, V. Azzolini, R. Barbieri, A. Baty, G. Bauer, R. Bi, S. Brandt, W. Busza, I. A. Cali, M. D'Alfonso, Z. Demiragli, G. Gomez Ceballos, M. Goncharov, P. Harris, D. Hsu, M. Hu, Y. Iiyama, G. M. Innocenti, M. Klute, D. Kovalskyi, Y.-J. Lee, A. Levin, P. D. Luckey, B. Maier, A. C. Marini, C. Mcginn, C. Mironov, S. Narayanan, X. Niu, C. Paus, C. Roland, G. Roland, G. S. F. Stephans, K. Sumorok, K. Tatar, D. Velicanu, J. Wang, T. W. Wang, B. Wyslouch, S. Zhaozhong

University of Minnesota, Minneapolis, USA

A. C. Benvenuti, R. M. Chatterjee, A. Evans, P. Hansen, S. Kalafut, Y. Kubota, Z. Lesko, J. Mans, S. Nourbakhsh, N. Ruckstuhl, R. Rusack, J. Turkewitz, M. A. Wadud

University of Mississippi, Oxford, USA

J. G. Acosta, S. Oliveros

University of Nebraska-Lincoln, Lincoln, USA

E. Avdeeva, K. Bloom, D. R. Claes, C. Fangmeier, F. Golf, R. Gonzalez Suarez, R. Kamalieddin, I. Kravchenko, J. Monroy, J. E. Siado, G. R. Snow, B. Stieger

State University of New York at Buffalo, Buffalo, USA

A. Godshalk, C. Harrington, I. Iashvili, D. Nguyen, A. Parker, S. Rappoccio, B. Roozbahani

Northeastern University, Boston, USA

G. Alverson, E. Barberis, C. Freer, A. Hortiangtham, A. Massironi, D. M. Morse, T. Orimoto, R. Teixeira De Lima, T. Wamorkar, B. Wang, A. Wisecarver, D. Wood

Northwestern University, Evanston, USA

S. Bhattacharya, O. Charaf, K. A. Hahn, N. Mucia, N. Odell, M. H. Schmitt, K. Sung, M. Trovato, M. Velasco

University of Notre Dame, Notre Dame, USA

R. Bucci, N. Dev, M. Hildreth, K. Hurtado Anampa, C. Jessop, D. J. Karmgard, N. Kellams, K. Lannon, W. Li, N. Loukas, N. Marinelli, F. Meng, C. Mueller, Y. Musienko[38], M. Planer, A. Reinsvold, R. Ruchti, P. Siddireddy, G. Smith, S. Taroni, M. Wayne, A. Wightman, M. Wolf, A. Woodard

The Ohio State University, Columbus, USA

J. Alimena, L. Antonelli, B. Bylsma, L. S. Durkin, S. Flowers, B. Francis, A. Hart, C. Hill, W. Ji, T. Y. Ling, W. Luo, B. L. Winer, H. W. Wulsin

Princeton University, Princeton, USA

S. Cooperstein, O. Driga, P. Elmer, J. Hardenbrook, P. Hebda, S. Higginbotham, A. Kalogeropoulos, D. Lange, J. Luo, D. Marlow, K. Mei, I. Ojalvo, J. Olsen, C. Palmer, P. Piroué, J. Salfeld-Nebgen, D. Stickland, C. Tully

University of Puerto Rico, Mayaguez, USA

S. Malik, S. Norberg

Purdue University, West Lafayette, USA

A. Barker, V. E. Barnes, S. Das, L. Gutay, M. Jones, A. W. Jung, A. Khatiwada, D. H. Miller, N. Neumeister, C. C. Peng, H. Qiu, J. F. Schulte, J. Sun, F. Wang, R. Xiao, W. Xie

Purdue University Northwest, Hammond, USA

T. Cheng, J. Dolen, N. Parashar

Rice University, Houston, USA

Z. Chen, K. M. Ecklund, S. Freed, F. J. M. Geurts, M. Guilbaud, M. Kilpatrick, W. Li, B. Michlin, B. P. Padley, J. Roberts, J. Rorie, W. Shi, Z. Tu, J. Zabel, A. Zhang

University of Rochester, Rochester, USA

A. Bodek, P. de Barbaro, R. Demina, Y. t. Duh, T. Ferbel, M. Galanti, A. Garcia-Bellido, J. Han, O. Hindrichs, A. Khukhunaishvili, K. H. Lo, P. Tan, M. Verzetti

The Rockefeller University, New York, USA

R. Ciesielski, K. Goulianos, C. Mesropian

Rutgers, The State University of New Jersey, Piscataway, USA

A. Agapitos, J. P. Chou, Y. Gershtein, T. A. Gómez Espinosa, E. Halkiadakis, M. Heindl, E. Hughes, S. Kaplan,
R. Kunnawalkam Elayavalli, S. Kyriacou, A. Lath, R. Montalvo, K. Nash, M. Osherson, H. Saka, S. Salur, S. Schnetzer,
D. Sheffield, S. Somalwar, R. Stone, S. Thomas, P. Thomassen, M. Walker

University of Tennessee, Knoxville, USA

A. G. Delannoy, J. Heideman, G. Riley, K. Rose, S. Spanier, K. Thapa

Texas A&M University, College Station, USA

O. Bouhali[75], A. Castaneda Hernandez[75], A. Celik, M. Dalchenko, M. De Mattia, A. Delgado, S. Dildick, R. Eusebi,
J. Gilmore, T. Huang, T. Kamon[76], R. Mueller, Y. Pakhotin, R. Patel, A. Perloff, L. Perniè, D. Rathjens, A. Safonov,
A. Tatarinov

Texas Tech University, Lubbock, USA

N. Akchurin, J. Damgov, F. De Guio, P. R. Dudero, J. Faulkner, E. Gurpinar, S. Kunori, K. Lamichhane, S. W. Lee,
T. Mengke, S. Muthumuni, T. Peltola, S. Undleeb, I. Volobouev, Z. Wang

Vanderbilt University, Nashville, USA

S. Greene, A. Gurrola, R. Janjam, W. Johns, C. Maguire, A. Melo, H. Ni, K. Padeken, J. D. Ruiz Alvarez, P. Sheldon,
S. Tuo, J. Velkovska, Q. Xu

University of Virginia, Charlottesville, USA

M. W. Arenton, P. Barria, B. Cox, R. Hirosky, M. Joyce, A. Ledovskoy, H. Li, C. Neu, T. Sinthuprasith, Y. Wang,
E. Wolfe, F. Xia

Wayne State University, Detroit, USA

R. Harr, P. E. Karchin, N. Poudyal, J. Sturdy, P. Thapa, S. Zaleski

University of Wisconsin-Madison, Madison, WI, USA

M. Brodski, J. Buchanan, C. Caillol, D. Carlsmith, S. Dasu, L. Dodd, S. Duric, B. Gomber, M. Grothe, M. Herndon,
A. Hervé, U. Hussain, P. Klabbers, A. Lanaro, A. Levine, K. Long, R. Loveless, V. Rekovic, T. Ruggles, A. Savin,
N. Smith, W. H. Smith, N. Woods

[†] **Deceased**

 1: Also at Vienna University of Technology, Vienna, Austria
 2: Also at IRFU, CEA, Université Paris-Saclay, Gif-sur-Yvette, France
 3: Also at Universidade Estadual de Campinas, Campinas, Brazil
 4: Also at Federal University of Rio Grande do Sul, Porto Alegre, Brazil
 5: Also at Universidade Federal de Pelotas, Pelotas, Brazil
 6: Also at Université Libre de Bruxelles, Brussels, Belgium
 7: Also at Institute for Theoretical and Experimental Physics, Moscow, Russia
 8: Also at Joint Institute for Nuclear Research, Dubna, Russia
 9: Also at Fayoum University, El-Fayoum, Egypt
10: Now at British University in Egypt, Cairo, Egypt
11: Also at Zewail City of Science and Technology, Zewail, Egypt
12: Now at Ain Shams University, Cairo, Egypt
13: Now at RWTH Aachen University, III. Physikalisches Institut A, Aachen, Germany
14: Also at Department of Physics, King Abdulaziz University, Jeddah, Saudi Arabia
15: Also at Université de Haute Alsace, Mulhouse, France
16: Also at Skobeltsyn Institute of Nuclear Physics, Lomonosov Moscow State University, Moscow, Russia
17: Also at Tbilisi State University, Tbilisi, Georgia
18: Also at CERN, European Organization for Nuclear Research, Geneva, Switzerland
19: Also at University of Hamburg, Hamburg, Germany
20: Also at Brandenburg University of Technology, Cottbus, Germany

21: Also at Institute of Nuclear Research ATOMKI, Debrecen, Hungary

22: Also at MTA-ELTE Lendület CMS Particle and Nuclear Physics Group, Eötvös Loránd University, Budapest, Hungary

23: Also at Institute of Physics, University of Debrecen, Debrecen, Hungary

24: Also at Indian Institute of Technology Bhubaneswar, Bhubaneswar, India

25: Also at Institute of Physics, Bhubaneswar, India

26: Also at Shoolini University, Solan, India

27: Also at University of Visva-Bharati, Santiniketan, India

28: Also at University of Ruhuna, Matara, Sri Lanka

29: Also at Isfahan University of Technology, Isfahan, Iran

30: Also at Yazd University, Yazd, Iran

31: Also at Plasma Physics Research Center, Science and Research Branch, Islamic Azad University, Tehran, Iran

32: Also at Università degli Studi di Siena, Siena, Italy

33: Also at INFN Sezione di Milano-Bicocca^a, Università di Milano-Bicocca^b, Milano, Italy

34: Also at International Islamic University of Malaysia, Kuala Lumpur, Malaysia

35: Also at Malaysian Nuclear Agency, MOSTI, Kajang, Malaysia

36: Also at Consejo Nacional de Ciencia y Tecnología, Mexico City, Mexico

37: Also at Warsaw University of Technology, Institute of Electronic Systems, Warsaw, Poland

38: Also at Institute for Nuclear Research, Moscow, Russia

39: Now at National Research Nuclear University 'Moscow Engineering Physics Institute' (MEPhI), Moscow, Russia

40: Also at Institute of Nuclear Physics of the Uzbekistan Academy of Sciences, Tashkent, Uzbekistan

41: Also at St. Petersburg State Polytechnical University, St. Petersburg, Russia

42: Also at University of Florida, Gainesville, USA

43: Also at P.N. Lebedev Physical Institute, Moscow, Russia

44: Also at California Institute of Technology, Pasadena, USA

45: Also at Budker Institute of Nuclear Physics, Novosibirsk, Russia

46: Also at Faculty of Physics, University of Belgrade, Belgrade, Serbia

47: Also at INFN Sezione di Pavia^a Università di Pavia^b, Pavia, Italy

48: Also at University of Belgrade, Faculty of Physics and Vinca Institute of Nuclear Sciences, Belgrade, Serbia

49: Also at Scuola Normale e Sezione dell'INFN, Pisa, Italy

50: Also at National and Kapodistrian University of Athens, Athens, Greece

51: Also at Riga Technical University, Riga, Latvia

52: Also at Universität Zürich, Zurich, Switzerland

53: Also at Stefan Meyer Institute for Subatomic Physics (SMI), Vienna, Austria

54: Also at Adiyaman University, Adiyaman, Turkey

55: Also at Istanbul Aydin University, Istanbul, Turkey

56: Also at Mersin University, Mersin, Turkey

57: Also at Piri Reis University, Istanbul, Turkey

58: Also at Izmir Institute of Technology, Izmir, Turkey

59: Also at Necmettin Erbakan University, Konya, Turkey

60: Also at Marmara University, Istanbul, Turkey

61: Also at Kafkas University, Kars, Turkey

62: Also at Istanbul Bilgi University, Istanbul, Turkey

63: Also at Rutherford Appleton Laboratory, Didcot, United Kingdom

64: Also at School of Physics and Astronomy, University of Southampton, Southampton, United Kingdom

65: Also at Monash University, Faculty of Science, Clayton, Australia

66: Also at Instituto de Astrofísica de Canarias, La Laguna, Spain

67: Also at Bethel University, St. Paul, USA

68: Also at Utah Valley University, Orem, USA

69: Also at Purdue University, West Lafayette, USA

70: Also at Beykent University, Istanbul, Turkey

71: Also at Bingol University, Bingol, Turkey

72: Also at Erzincan University, Erzincan, Turkey

73: Also at Sinop University, Sinop, Turkey

74: Also at Mimar Sinan University, Istanbul, Istanbul, Turkey

75: Also at Texas A&M University at Qatar, Doha, Qatar

76: Also at Kyungpook National University, Daegu, Korea